

ABSTRACT OF THESIS

-----

A COMPARISON OF THE SEDIMENTATION DIAMETER  
AND THE SIEVE DIAMETER  
FOR VARIOUS TYPES OF NATURAL SANDS

Submitted by  
Eugene F. Serr III

In partial fulfillment of the requirements  
For the Degree of Master of Science  
in Irrigation Engineering  
Colorado A & M College  
Fort Collins, Colorado

March 1948

378.788

A0

1948

1a

A COMPARISON OF THE SEDIMENTATION DIAMETER AND THE  
SIEVE DIAMETER FOR VARIOUS TYPES OF NATURAL SANDS

ABSTRACT

Introduction

Sand, silt, and gravel, together classed as sediment by the hydraulic engineer, present problems of vital importance in projects for irrigation, navigation, soil conservation, flood control, and water power development. High costs of maintenance, loss of efficiency, and often complete destruction of important engineering works have been experienced due to filling of reservoirs by sediment, filling or scouring in navigation and irrigation channels, and erosion and gullyng on arable lands. These problems have received considerable study both in the field and laboratory, offering a very active field at the present time; but progress remains insignificant in comparison to the problems.

Most of the research in this field is still in the stage of development of satisfactory equipment and techniques for the measurement of the sediment load in streams. The next stage is improvement in the methods of analyzing sediment samples.

Nearly all studies of coarse sediments, particles larger than about 1/16 millimeters in diameter, are made on the basis of the sieve analysis, since this is the most convenient and reproducible procedure available. It is generally recognized, however, that the fundamental property governing the motion of a sediment particle in a fluid is not its size, but its settling velocity, a function of its volume, shape, density, and the properties of the fluid. The established equation for the vertical distribution of sediment in a stream involves the mean settling velocity as the parameter describing the particles. It has been a common practice to use the mean sieve diameter in computing this mean settling velocity. The purpose of this study is to show the magnitude of error involved in this procedure and to present a practical method of estimating the mean fall velocity with greater accuracy.

A recent standardization of terms by a special subcommittee on sediment terminology of the Stream Dynamics Committee of the American Geophysical Union defines three distinct diameters of a particle as follows:

Sieve diameter -- The size of sieve opening through which the given particle will just pass.

Nominal diameter -- The diameter of a sphere of the same volume as the given particle.

Sedimentation diameter -- The diameter of a sphere of the same specific gravity and the same terminal uniform settling velocity as the given particle in the same sedimentation fluid.

A comparison of the sedimentation diameter and the sieve diameter for various sands, including graphs of these two diameters plotted against each other for various types of sands, will accomplish the purpose of this study. Thus the problem to be answered in this report may be stated as follows: How do the sieve diameter and the sedimentation diameter vary in different sizes and types of sands?

#### Materials and procedure

Ten different sands from a wide variety of sources were used in this study to assure a wide range of particle shapes. The sieve analysis of each sand was made using screen numbers 10 to 100 (Tyler Standard Screen Scale) for a 15 minute period in a Rotap Shaker. The cumulative sieve analysis curve for each sand is shown in the Appendix.

Minute samples of 50 random particles were split out of the sieve fractions for individual fall velocity measurements using a settling tube and stopwatch. The mean settling velocity in water, and the standard deviation from the mean, were computed from

the values obtained for the 50 random particles. The water temperature was recorded for each series of velocity measurements. A specific gravity determination was made on each sieve fraction.

Assuming the mean nominal diameter equal to the mean sieve diameter, all data necessary for the determination of the mean sedimentation diameter of each sieve fraction was then available. This graphical determination is presented in detail in the thesis. The cumulative distribution curve of sedimentation diameters is plotted on the same graph as the sieve analysis for comparison.

Magnified photographs of the sieve fractions are presented to show the particle shapes involved.

#### Analysis of data

In comparing the two distribution curves (sieve analysis and hydraulic analysis), it was first noted that the sieve diameter was always larger than the sedimentation diameter. The average sieve diameter at the geometric mean size was 23.7% larger than the sedimentation diameter for the ten sands. The individual differences varied from 14.4% for the highly spherical dune sand studied to 39.0% for the angular talus debris studied.

An important characteristic noted in the comparison of the two analysis curves was the wider deviation of the two values in the coarser range. The ratio of the sedimentation diameter to the sieve diameter was seen to decrease consistently from nearly unity at the 100 mesh size (0.161 millimeters average) to about 0.50 at the 8 mesh size (2.844 millimeters average).

The sedimentation diameter is plotted both arithmetically and logarithmically against the sieve diameter. In both cases a family of curves is obtained, each curve representing a particular sand. These curves show the relative importance of size and shape in determining the sedimentation diameter. The most angular sand studied gave sedimentation diameters 10% to 20% smaller than the sedimentation diameters for the corresponding sieve fractions of the most spherical sands studied. Over most of the range studied, a size increase of 20% effected the same difference in sedimentation diameter as a shape change from the least spherical to the most spherical of the sands studied.

A procedure is presented for using the graphs in estimating the mean sedimentation diameter and fall velocity of a sand when the mean sieve diameter and the degree of sphericity relative to the sands of this study are known.

## Conclusions

A detailed comparison of the sedimentation diameter and the sieve diameter for the range of sediment particle sizes 0.15 to 1.65 millimeters (10 to 100 meshes to the inch, Tyler Standard Screen Scale) and for particle shapes ranging from a highly spherical dune sand to a highly angular talus debris sand has been completed in this study. A procedure for estimating the mean sedimentation diameter and the corresponding fall velocity in water at any temperature is included.

General conclusions of the study can be summarized as follows:

1. The family of sedimentation diameter versus sieve diameter curves for sands is asymptotic to the line on which these values are equal, in the direction of the origin. For practical purposes the difference between the two values becomes negligible for all sands at about 0.05 millimeters. This confirms this value as the diameter of the coarsest particle for which the fall velocity in water at normal temperature can be calculated by Stokes equation (based on viscous resistance only).

2. The ratio of the sedimentation diameter decreases consistently in all sands from practically unity at sieve diameter values of 0.05 millimeters to about 0.50 at sieve diameter values of 2.84 millimeters (the average for the 6 to 8 mesh fraction, Tyler Standard Screen Scale).

3. The sedimentation diameter values for the most angular sand studied (talus debris) varied from 10% to 20% smaller than the sedimentation diameter values of the most spherical of the dune and river bed sands of corresponding sieve fractions.

LIBRARY  
COLORADO A. & M. COLLEGE  
FORT COLLINS

LIBRARY  
COLORADO A. & M. COLLEGE  
FORT COLLINS COLORADO

T H E S I S

-----

A COMPARISON OF THE SEDIMENTATION DIAMETER  
AND THE SIEVE DIAMETER  
FOR VARIOUS TYPES OF NATURAL SANDS

Submitted by  
Eugene F. Serr III

In partial fulfillment of the requirements  
For the Degree of Master of Science  
in Irrigation Engineering  
Colorado A & M College  
Fort Collins, Colorado

March, 1948

LIBRARY  
COLORADO A. & M. COLLEGE  
FORT COLLINS, COLORADO

TA  
710  
.5427  
1948

COLORADO AGRICULTURAL AND MECHANICAL COLLEGE

37875  
A D  
1948

.....MARCH.....1948.....

I HEREBY RECOMMEND THAT THE THESIS PREPARED UNDER MY  
SUPERVISION BY.....EUGENE F. SERR III.....

ENTITLED.....A COMPARISON OF THE SEDIMENTATION  
DIAMETER AND THE SIEVE DIAMETER FOR VARIOUS  
.....TYPES OF NATURAL SANDS.....

BE ACCEPTED AS FULFILLING THIS PART OF THE REQUIREMENTS FOR THE  
DEGREE OF MASTER OF.....SCIENCE.....

MAJORING IN.....IRRIGATION ENGINEERING.....

CREDITS 5.....

*W A Christensen*  
In Charge of Thesis

APPROVED *Robert L Lewis*  
Head of Department

Examination Satisfactory

Committee on Final Examination

*Robert L Lewis* *W A Christensen*  
*Willard Eddy* *Andrew S. Clark*  
*Robert O. Bock*

*David H Morgan*  
Dean of the Graduate School

Permission to publish this thesis or any part of it  
must be obtained from the Dean of the Graduate School.

## ACKNOWLEDGEMENTS

The writer is indebted to Dr. N. A. Christensen, Dean of Engineering, Colorado A & M College, for invaluable assistance in the preparation of this thesis.

Special acknowledgement is also due Dr. R. O. Bock, Professor of Physics, Colorado A & M College, for assistance in the preparation of the magnified photographs of the sands.

## TABLE OF CONTENTS

Chapter		Page
I	INTRODUCTION . . . . .	6
	The problem . . . . .	8
II	REVIEW OF LITERATURE . . . . .	10
III	MATERIALS AND PROCEDURE. . . . .	14
IV	ANALYSIS OF DATA . . . . .	20
V	CONCLUSIONS. . . . .	35
	APPENDIX . . . . .	38
	BIBLIOGRAPHY . . . . .	81

## LIST OF TABLES AND FIGURES

	Page
Table 1	Types and Sources of the Sand Studied. . . . . 15
Table 2	Computation of the Sedimentation Diameter. . . . . 21
Figure 1	Dimensionless Plot of Experimental Data. . . . . 25
Figure 2	Variation of Sedimentation Diameter with Sieve Diameter . . . . . 30
Figure 3	Variation of Sedimentation Diameter with Sieve Diameter (Logarithmic) . 32

Chapter I  
INTRODUCTION

Sand, silt, and gravel, together classed as sediment by the hydraulic engineer, present problems of vital importance in projects for irrigation, navigation, soil conservation, flood control, and water power development. High costs of maintenance, loss of efficiency, and often complete destruction of important engineering works have been experienced due to filling of reservoirs by sediment, filling or scouring in navigation and irrigation channels, and erosion and gullying on arable lands. These problems have received considerable study both in the field and laboratory, offering a very active field at the present time; but progress remains insignificant in comparison to the problems. An additional alarming feature of the sediment problems is that they may be expected to become even more serious in the future in view of the extensive industrial, commercial, and public service development of streams accomplished in recent years. A great deal of fundamental study remains before hydraulic engineers can hope to predict satisfactorily the behavior of sediments in order to control them.

Most of the research in this field is still in the stage of development of satisfactory equipment and techniques for the measurement of the sediment load in streams. The next stage is improvement in the methods of analyzing sediment samples. It is generally recognized that the fundamental property governing the motion of a sediment particle in a fluid is not its size, but its settling velocity, a function of its volume, shape, density, and the properties of the fluid. Yet nearly all studies of coarse sediments, particles larger than about 1/16 millimeter in diameter, are made on the basis of the sieve analysis since this is the most convenient and reproducible procedure available. This thesis is a study of the shape factor ignored in this procedure.

A recent standardization of terms by a special subcommittee on sediment terminology of the Stream Dynamics Committee of the American Geophysical Union (1) defines three distinct diameters of a particle as follows:

Sieve diameter -- The size of sieve opening through which the given particle will just pass.

Nominal diameter -- The diameter of a sphere of the same volume as the given particle.

Sedimentation diameter -- The diameter of a sphere of the same specific gravity and the same terminal uniform settling velocity as the given particle in the same sedimentation fluid.

The value of the sedimentation diameter lies in the fact that it is a measure of the settling velocity but does not entail specification of (1) a certain fluid temperature (fixing a particular viscosity and density) and (2) a certain particle density. Stated more significantly, this means that for a given particle volume, the sedimentation diameter is a function of the particle shape alone. A comparison of the sedimentation diameter and the sieve diameter for various sands is needed.

#### The problem

The problem to be answered in this report may be stated as follows: How do the sieve diameter and the sedimentation diameter vary in different sizes and types of sands? In analysis of the problem, the following questions arise:

1. How can the distribution curve of sedimentation diameters be determined for the sands to be studied?
2. What is the nature of the resistance curves (drag coefficient versus Reynolds number) for various sands?
3. To what extent does this report support the studies showing that the sphericity of sand particles generally increases with size?

4. What is the nature of the curves of sedimentation diameter versus sieve diameter for various sands?

5. How does the ratio of the sedimentation diameter to the sieve diameter vary as the sieve diameter increases?

6. What difference in sedimentation diameter may be expected for the same sieve fraction of sands of different degrees of sphericity?

The study will be limited to sands of sieve diameters corresponding generally to sieves 10 to 100 meshes to the inch (Tyler Standard Screen Scale). These screens have openings from 1.651 to 0.147 millimeters in diameter. This range includes the fine, medium, and coarse sands as defined in the terminology report referred to earlier (1). The particle shapes to be studied will range from a highly angular talus debris sand to a highly spherical dune sand. Ten sands from as widely varying sources as possible will be sampled for this study.

Chapter II  
REVIEW OF LITERATURE

The metallurgical engineers concerned with ore-dressing problems were among the first to be concerned with the problem of relating the sieve size and fall velocity of mineral particles in water. Richards (3), in 1908, made an extensive experimental study of the settling velocities of crushed quartz and galena grains of a large number of sieve fractions (average diameters of 0.32 to 11.93 millimeters). This investigator found that the "friction factor" in "Rittenger's formula" (proportional to the drag coefficient of the drag force equation) was practically constant for grains larger than 1.55 millimeters in diameter. The difference between this factor for the quartz and the galena grains was attributed solely to the differences in the specific gravities of the minerals. The possibility of a shape factor difference was entirely overlooked in this early investigation.

Rubey (5), using Richards' data, developed a formula in 1933 which followed these results reasonably well. This formula was essentially a superposition of

Stokes equation, applicable to the purely viscous range, and the drag force equation for the "impact range" (referring to the range in which the drag coefficient is practically independent of the viscous forces). This was claimed to be a general formula for gravel, sand, and silt particles. Thus even at this late date the importance of the shape factor was not realized.

Among the first to emphasize the importance of the shape factor was a Russian investigator, Zegrzda (9:52-54), in 1934. Zegrzda plotted original experimental data, and other data available, in the drag coefficient versus Reynolds number graph. He divided the band of experimental points into three stages -- the "streamline stage" (Stokes range), the intermediate stage, and the "turbulent stage" (drag coefficient essentially constant). The intermediate stage is further divided into two ranges in which different empirical relations seemed to hold. Empirical formulas relating the drag coefficient and the Reynolds number for the two curves limiting the spread of the experimental points are presented for each limited range. The solution for the true fall velocity, using these formulas, involves a tedious trial and error process. Their practical value is questionable. An additional weakness of this presentation lies in the fact that the

sands studied are not shown or described sufficiently to give a picture of the relative degrees of sphericity involved.

Wadell (7), defined the true sphericity as the ratio of the surface of a sphere of the same volume as the particle to the actual surface area of the particle. He analyzes the experimental data on extremely thin steel disks (sphericity values of 0.12 and 0.22) and shows graphically the wide spread between the resistance curves for these disks and that for spheres, even in Stokes range. Wadell was the first to show that elimination of the nominal diameter between Reynolds number and the drag coefficient,

$$R = \frac{\rho_f v_0 d_n}{\mu} \quad (1)$$

$$C_D = \frac{4}{3} \frac{(\rho_s - \rho_f) g d_n}{v_0^2 \rho_f} \quad (2)$$

yields a series of lines,

$$C_D/R = \frac{4}{3} \frac{(\rho_s - \rho_f) g \mu}{\rho_f^2 v_0^3}$$

$$\text{or } \log C_D = \log R + \log \left( \frac{4}{3} \frac{(\rho_s - \rho_f) g \mu}{\rho_f^2 v_0^3} \right) \quad (3)$$

on the logarithmic  $C_D$  versus  $R$  graph, each of which represents a particular terminal uniform settling velocity ( $v_0$ ) in the same fluid. He was also the first to suggest the definition of sedimentation diameter as now accepted. His excellent theoretical study is of little practical value to the "sediment engineers", however, since the sphericities of natural particles

are much greater than those of the disks in the studies analyzed.

Heywood (6:27-28, 40-47), in a detailed study of particle shape and fall velocity, considers a volume constant,  $\underline{k}$ , defined as follows:

$$k = \frac{\text{volume of particle}}{d^3}$$

where  $d$  is defined as the diameter of a circle of area equal to the projected area of the particle when placed in its most stable position. The volume constant,  $\underline{k}$ , varies from  $\pi/6$  for a sphere to values of less than 0.1. Heywood presents a graphical procedure for determining the fall velocity for different values of  $\underline{k}$ . This is the most practical procedure available for estimating the fall velocity with consideration for particle shape. However, the estimation of the shape factor  $\underline{k}$  is very indefinite.

A study of the resistance curves for definite sands, pictured in enlarged photographs, is the straightforward approach needed to this problem. A comparison of corresponding sedimentation and sieve diameters for sands thus studied seems the best method of presenting the results for practical use.

Table 1.--TYPES AND SOURCES OF THE SANDS STUDIED.

SAMPLE NUMBER	TYPE	SOURCE
1	River bed material	Cache la Poudre River, Fort Collins, Colorado.
2	River bed material	Michigan River, Camp Pennock, Colorado.
3	Fine rock debris	Talus slide, Verdi, Nevada.
4	Dune sand	Small dunes, Fernley, Nevada.
5	River bed material	Truckee River, Truckee, California.
6	River bed material	South Fork Yuba River, Cisco, California.
7	River bed material	Putah Creek, Davis, California.
8	Dune sand	Dunes near Great Salt Lake, Utah.
9	Lake beach material	Grand Lake, Colorado.
10	River bed material	Cache la Poudre River, Chambers Lake, Colorado.

## Chapter III

### MATERIALS AND PROCEDURE

The sands used in this study were collected from a variety of sources in order to assure a wide range of shapes. Table 1 lists the sands and their sources. The cumulative sieve analysis curve for each of these sands is shown in Appendix B together with the hydraulic analysis curve.

New sieves of the Tyler Standard Screen Scale were used in a Ro-tap Shaker for this study. Tyler Numbers 10, 14, 20, 28, 35, 48, 60, 65, 80, and 100 were used, with some exceptions (Appendix A). Material coarser than the coarsest fraction to be obtained was first removed from the oven dried and air-cooled raw sample. Five hundred grams were quartered out for the analysis. The shaking time used was 15 minutes. Each sieve fraction was weighed, and those greater than 10 grams were kept in separate containers for the settling velocity analysis.

Minute samples of 50 random particles to be used for individual fall velocity measurements were prepared for the sieve fractions with the aid of a

microsplit constructed in accordance with the specifications set forth by Otto (2). Each particle was timed through a fall of 50 centimeters in a glass settling tube full of water. The diameter of the settling tube was 5.08 centimeters, giving ratios of particle diameters to boundary width less than 0.06 in all cases. Thus this study involves no appreciable boundary influence on the settling velocities.

In all cases the particle fell about 25 centimeters through the water before the timed interval started to insure the establishment of the terminal uniform settling velocity and to avoid effects of the air water interface. A stop watch with a ten-second sweep gave readings to 0.01 second in these velocity measurements. The temperature of the water in the center of the tube halfway down the timed settling distance was recorded at the beginning and end of each group of measurements. These temperature recordings were averaged for the purpose of the computations. No series of measurements were used when the two temperature recordings differed by more than  $1.0^{\circ}$  Fahrenheit. The temperature just outside the tube was also kept within  $1.0^{\circ}$  Fahrenheit to insure that the transverse viscosity pattern in the tube was sufficiently plane to insure the desired accuracy.

The average settling velocity of each sieve fraction was computed from the values obtained for the 50 random particles. The standard deviation of the fall velocities from the mean was also computed for each sieve fraction.

To determine the particle density of the fraction, about 25 cubic centimeters of a fraction were used. This was poured into a tared 100 milliliter volumetric flask. The flask plus the oven dried sample was weighed to the nearest milligram on the analytical balance. The flask was then filled with water, stopped, and inverted several times. The flask was left standing approximately 10 minutes before agitating severely to insure the escape of all minute air bubbles. The meniscus was then adjusted exactly to the mark with the aid of an eye dropper. The flask was weighed again on the balance with its sand and water content. Finally, the temperature of the water at the time of weighing was recorded to the nearest  $0.1^{\circ}$  Fahrenheit.

The steps in the computation of the particle density are outlined:

1. The weight of the water added to the volumetric flask was converted to volume by dividing by the water density as determined from a temperature-density curve.

represent a constant velocity, the intersection of such lines, drawn through the experimental points ( $R, C_D$ ), with the curve for spheres gives  $R_0$  and  $C_{D_0}$  values corresponding to the mean sedimentation diameters of the sieve fractions. The ratio  $C_{D_0}/C_D$  will then be the ratio of the sedimentation diameter to the sieve diameter for the sieve fraction, from which the sedimentation diameter is easily obtained.

The cumulative distribution curve of sedimentation diameters (Appendix B) was constructed by plotting the average cumulative percentage values of the sieve fractions against the mean sedimentation diameters of the fractions as determined.

The magnified photographs of the sieve fractions (Appendix C) were taken with side lighting adjusted to show the surface detail of the particles as well as possible. A regrettable 20% loss of detail was incurred in the printing of the sheets as shown.

2. The solid volume of the particles was determined by the volume of the water added from the volume of the flask.

3. The density of the particles was determined by dividing the weight of the sample by the solid volume as determined in step 2.

The reason for presenting this simple procedure in such detail is that the values obtained differ from those usually assumed in the following respects:

1. The density values obtained were generally considerably less than that of quartz (2.65 grams per cubic centimeter), averaging about 2.60 grams per cubic centimeter.

2. The difference between the particle densities of the different fractions of a given sand was often of appreciable magnitude (Appendix A).

Using the average sieve diameter ( $\bar{d}$ ), and the average velocity ( $\bar{v}_0$ ), the mean Reynolds number ( $R$ ) and drag coefficient ( $C_D$ ) were computed for each sieve fraction as follows:

$$R = \frac{\rho_f \bar{v}_0 \bar{d}_n}{\mu} \quad (4)$$

$$C_D = \frac{4}{5} \frac{(\rho_s - \rho_f) g \bar{d}_n}{\bar{v}_0^2 \rho_f} \quad (5)$$

These points ( $R$ ,  $C_D$ ) were plotted on the logarithmic  $R$  versus  $C_D$  graph together with the established curve for spheres. Since lines of +1 slope on this graph

Chapter IV  
ANALYSIS OF DATA

The experimental data are presented in Appendix A. Using these data, the mean Reynolds number ( $R$ ) and drag coefficient ( $C_D$ ) were determined for each sieve fraction on which the hydraulic analysis was made. The values obtained are shown in the third and fourth columns of Table 2. In Figure 1 these  $R$  and  $C_D$  values are plotted together with the curve for spheres.

Dimensional analysis of the drag on immersed bodies yields the three parameters -- Reynolds number, drag coefficient, and shape. Thus the drag coefficient is a function of Reynolds number and shape:

$$C_D = \phi ( R, \text{shape} ) \quad (6)$$

With the  $C_D$  versus  $R$  curve for perfect spheres established from a wealth of experimental data, it follows that all bodies with less hydraulic shape efficiency than perfect spheres will yield points falling above this curve. Only bodies of greater shape efficiency than spheres, that is, streamlined bodies, will yield points below the curve. Figure 1 shows that all of the experimental points of this study fall above the curve, with the exception of several points to the left of  $R = 6$ .

Table 2.--COMPUTATION OF SEDIMENTATION DIAMETER  $d_o$ .

$d$	Sand	R	$C_D$	$C_{D_o}$	$d_o/d$	$d_o$
0.161	1	3.64	8.09	8.59	1.062	0.171
0.161	2	3.54	8.80	9.00	1.023	0.165
0.161	4	3.40	10.2	11.07	0.921	0.148
0.178	8	5.16	6.64	6.74	1.016	0.180
0.178	10	4.89	7.43	7.28	0.980	0.174
0.192	4	4.95	8.29	7.59	0.915	0.175
0.192	5	4.79	8.64	7.83	0.906	0.174
0.227	1	6.71	6.48	6.00	0.926	0.210
0.227	2	6.81	6.70	6.04	0.901	0.205
0.227	3	5.03	10.23	8.28	0.810	0.184
0.227	4	7.24	6.73	5.89	0.875	0.199
0.227	5	6.28	8.54	6.93	0.811	0.184
0.252	6A	8.48	5.79	5.13	0.886	0.223
0.252	6B	8.10	6.45	5.51	0.854	0.215
0.252	8	10.60	4.66	4.32	0.927	0.233
0.252	9	9.68	4.73	4.50	0.951	0.239
0.252	10	9.16	6.00	5.08	0.846	0.213
0.270	1	9.05	5.78	5.03	0.870	0.235
0.270	2	10.07	5.11	4.58	0.896	0.242
0.270	3	8.36	6.13	5.34	0.871	0.236
0.270	4	7.24	6.73	5.89	0.875	0.199
0.270	5	9.22	6.30	5.16	0.819	0.222

Table 2.--COMPUTATION OF SEDIMENTATION DIAMETER  $d_o$ .--continued.

d	Sand	R	$C_D$	$C_{D_o}$	$d_o/d$	$d_o$
0.356	1	17.4	3.41	3.12	0.915	0.326
0.356	2	17.4	3.69	3.21	0.870	0.310
0.356	3	14.3	4.68	3.83	0.819	0.292
0.356	4	19.2	3.17	2.92	0.921	0.328
0.356	5	16.8	4.54	3.54	0.780	0.278
0.356	6A	16.7	4.18	3.43	0.821	0.292
0.356	6B	17.4	3.90	3.28	0.841	0.299
0.356	7	20.6	3.07	2.81	0.915	0.326
0.356	8	20.1	3.63	3.01	0.829	0.295
0.356	9	18.3	3.65	3.15	0.863	0.307
0.356	10	19.7	3.55	3.01	0.848	0.302
0.503	1	35.8	2.48	2.09	0.843	0.424
0.503	2	33.7	2.74	2.22	0.810	0.407
0.503	3	25.3	4.24	2.94	0.693	0.348
0.503	4	32.0	3.14	2.38	0.758	0.381
0.503	5	33.5	3.08	2.33	0.756	0.380
0.503	6A	36.6	2.46	2.06	0.837	0.421
0.503	6B	40.4	2.36	1.98	0.839	0.422
0.503	7	37.4	2.47	2.05	0.830	0.417
0.503	8	38.0	2.46	2.04	0.829	0.417
0.503	9	39.5	2.38	1.99	0.836	0.421
0.503	10	37.9	2.49	2.07	0.831	0.418

Table 2.--COMPUTATION OF SEDIMENTATION DIAMETER  $d_o$ .--continued.

$d$	Sand	R	$C_D$	$C_{D_o}$	$d_o/d$	$d_o$
0.712	Ottawa	83.3	1.35	1.26	0.933	0.664
0.712	1	68.1	1.93	1.53	0.792	0.564
0.712	2	65.2	2.09	1.60	0.765	0.545
0.712	3	59.1	2.21	1.69	0.764	0.544
0.712	4	60.7	2.31	1.70	0.736	0.524
0.712	5	61.0	2.48	1.73	0.697	0.496
0.712	6A	74.9	1.66	1.41	0.849	0.605
0.712	6B	75.6	1.86	1.45	0.779	0.554
0.712	7	67.8	2.06	1.56	0.757	0.539
0.712	9	75.9	1.76	1.43	0.812	0.578
0.712	10	72.7	1.88	1.48	0.787	0.560
1.001	1	125.4	1.56	1.16	0.744	0.744
1.001	2	125.6	1.57	1.16	0.739	0.739
1.001	3	105.3	1.95	1.32	0.677	0.677
1.001	6A	129.2	1.57	1.15	0.732	0.732
1.001	6B	143.5	1.40	1.06	0.757	0.757
1.001	7	122.2	1.70	1.20	0.706	0.706
1.001	9	133.3	1.63	1.15	0.705	0.705
1.001	10	135.0	1.48	1.11	0.750	0.750
1.410	2	213.	1.51	0.964	0.638	0.899
1.410	3	186.1	1.77	1.06	0.599	0.844
1.410	6A	222.	1.47	0.940	0.639	0.901

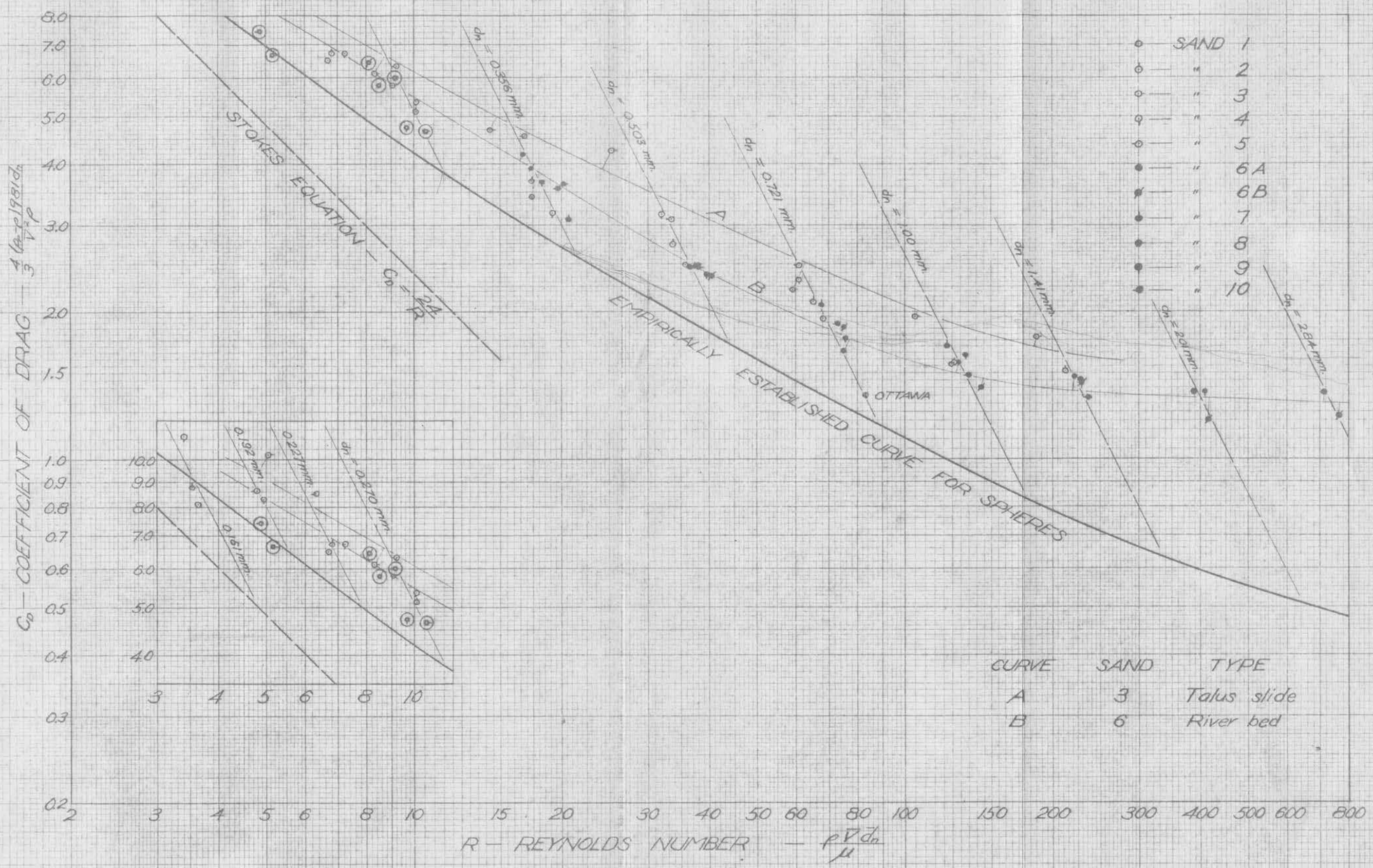
Table 2.--COMPUTATION OF SEDIMENTATION DIAMETER  $d_o$ .--continued.

d	Sand	R	$C_D$	$C_{D_o}$	$d_o/d$	$d_o$
1.410	6B	229.	1.44	0.915	0.635	0.895
1.410	9	228.	1.45	0.924	0.637	0.898
1.410	10	236.	1.34	0.893	0.666	0.939
2.006	6A	387.	1.37	0.765	0.539	1.12
2.006	6B	417.	1.20	0.713	0.594	1.19
2.006	9	408.	1.38	0.753	0.547	1.10
2.844	6A	657.	1.37	0.648	0.473	1.35
2.844	6B	634.	1.23	0.620	0.504	1.44

It is not inconceivable that these could represent streamlined sand particles, but examination of the magnified photographs of Appendix C rules out this possibility. The discrepancy must be ascribed to experimental error.

Curves representing constant geometric shapes on the  $C_D$  versus  $R$  graph are known as resistance curves. Strictly speaking, a natural sand cannot yield a resistance curve since it has been shown (8) that the larger particles of a sand generally exhibit greater sphericity than the smaller particles. The magnified photographs of the sands used in this study (Appendix C) support this general conclusion. Curves A and B of Figure 1 will be referred to as resistance curves for the particular sands represented as distinguished from resistance curves for constant geometric shapes.

The resistance curve for the least spherical of the sands studied (talus debris, Sample 3) was expected to lie farthest above the curve for spheres. Curve A (Figure 1) joins the points representing the fractions of this sand and falls above the other points. The points representing the dune sand (Sample 8) with particles nearly spherical in shape (Appendix C) fall generally below the others. The paucity of size fractions available in this sand renders construction of



CURVE	SAND	TYPE
A	3	Talus slide
B	6	River bed

FIG. 1. DIMENSIONLESS PLOT OF EXPERIMENTAL DATA

a resistance curve indefinite. Unfortunately, this applies to most of the sands studied, which explains the drawing of only two of the ten resistance curves. Curve B represents a river bed sand (Sample 6). The experimental points establishing this curve fall approximately in the center of the spread of the points representing the several river bed sands studied, and can be considered typical of these.

The flattening of the resistance curves at a nominal diameter ( $d_n$ ) value of about 1.5 millimeters indicates that this is near the size where viscous effects become secondary and the drag coefficient becomes independent of Reynolds number for natural particles. For spheres this does not occur until the diameter is about 5 millimeters.

The lines of constant nominal diameter ( $d_n$ ) in Figure 1 are shown in order to evaluate the assumption that the sieve diameter and nominal diameter are equal. This assumption was necessary in this study since no practical method is known for measuring the true nominal diameter of sand particles. The scatter of the experimental points about these lines is due principally to the deficiency of this assumption. Differences in particle densities and fluid properties cause some secondary scatter. An average of the particle densities

and the fluid properties determined in the experiments was used to establish the lines of constant nominal diameter.

The points are seen to scatter more in the smaller sizes. The scatter is a function of sphericity since only spheres would have equal nominal and sieve diameters. Thus the decreasing scatter in the larger sizes supports the observation that the larger sizes tend to be more spherical.

The procedure for the graphical determination of the sedimentation diameter ( $d_o$ ), using Figure 1, has been outlined earlier in this report. The values obtained are shown in the last column of Table 2. The table is arranged by mean sieve diameters (averages of the two openings limiting the fraction) to facilitate comparison of the sedimentation diameters for the different sands.

The two cumulative distribution curves from the mechanical analysis and the hydraulic analysis of each sand are presented in Appendix B. In comparing the two distribution curves, it is first noted that the sieve diameter ( $d$ ) is always larger than the sedimentation diameter ( $d_o$ ). An important characteristic noted is the wider deviation of the two values in the coarser range. In the sixth column of Table 2 the ratio  $d_o/d$  is

seen to decrease consistently from nearly unity at the 100 mesh size (0.161 millimeters average) to about 0.50 at the 8 mesh size (2.844 millimeters average). This consistent decrease in the  $d_o/d$  ratio is seen graphically in Figure 2.

Figure 2 shows the relative importance of size and shape in determining the fall velocity, that is, sedimentation diameter of natural sands. It is seen that the most angular sand (talus debris, Sample 3) gave sedimentation diameters 10% to 20% smaller than the sedimentation diameters of the most spherical sands studied. Looking into the data of Appendix A, it is seen that this corresponds to a 20% to 30% reduction in fall velocity. Over most of the range studied it is apparent that a size increase of approximately 20% would effect the same difference in sedimentation diameter and fall velocity as a shape change from the least spherical to the most spherical of the sands studied.

Figure 2 also shows that the  $d_o$  versus  $d$  curves are asymptotic to the line of  $d_o = d$  in the direction of the origin. For practical purposes, the difference between the two values becomes negligible for all sands at about  $d = 0.05$  millimeters. This is about the upper limit of Stokes range where viscous

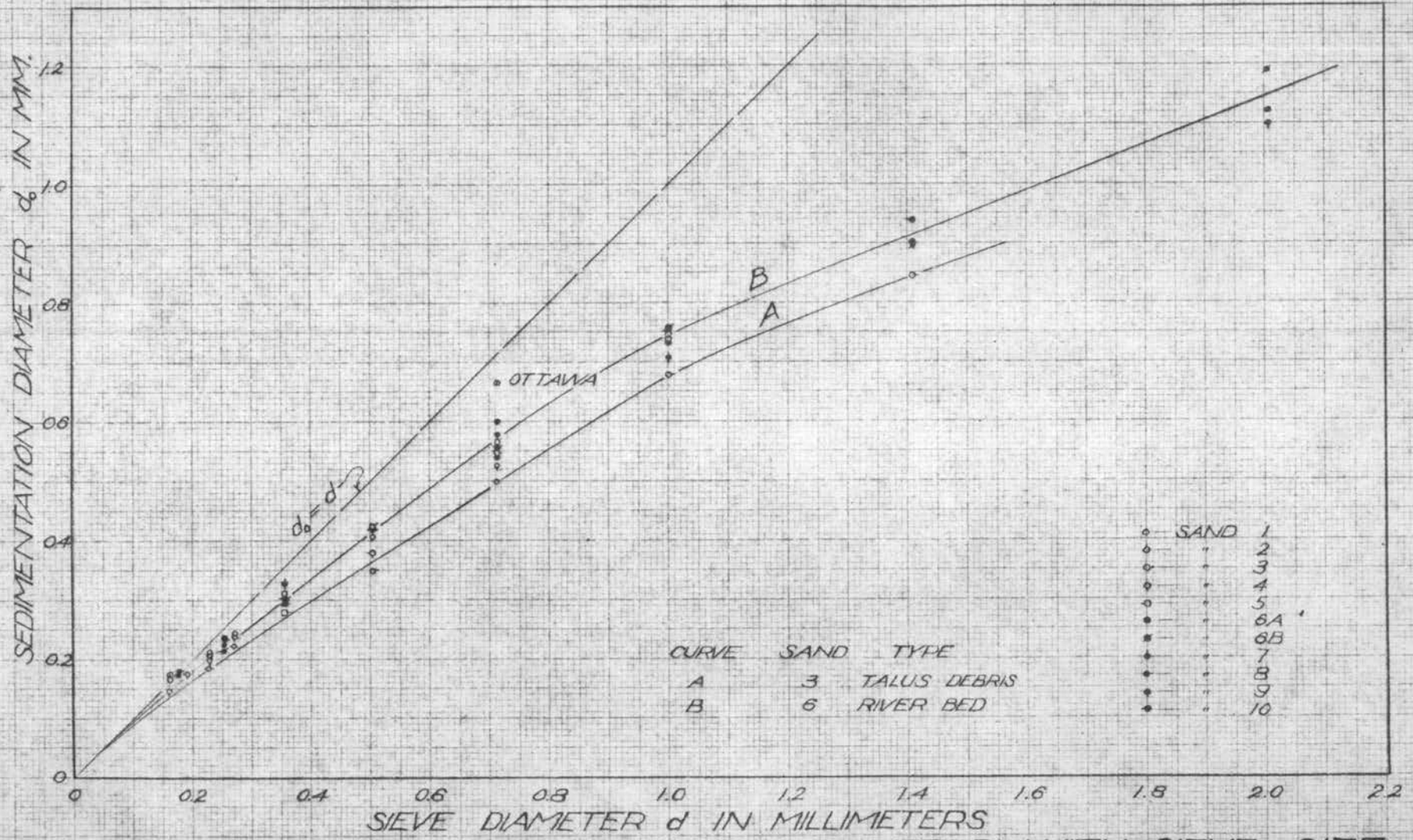


FIG. 2. VARIATION OF SEDIMENTATION DIAMETER WITH SIEVE SIZE

forces dominate and particle shape, within the normal range, has negligible effect upon the fall velocity. This establishes the largest size at which settling rate analysis of the silts and clays can be combined with mechanical analysis of the coarser range of a composite sediment sample to yield a continuous analysis curve. This supports the choice of the 200 mesh sieve (0.074 millimeters) as the finest screen practicable in the laboratory.

In Figure 3,  $d_0$  is plotted logarithmically against  $d$  to spread the data in the finer range. If the points falling above the line are omitted as erroneous through experimental error, the results indicate a family  $d_0$  versus  $d$  curves, for  $d$  values less than 0.8 millimeters, of the exponential form:

$$d_0 = K d^n \quad (7)$$

The factor  $K$  varies from 0.65 for the least spherical sand to 0.80 for the most spherical sand, and  $n$  varies from 0.87 to 0.93 for the same sands.

Sample 6 was chosen for the complete re-analysis to indicate the experimental error involved in this study. This sample was chosen for the wide size range it offered. The data from the two analyses are found in Appendix A. The plot of the two sets of data in the cumulative curves are shown in Appendix B.

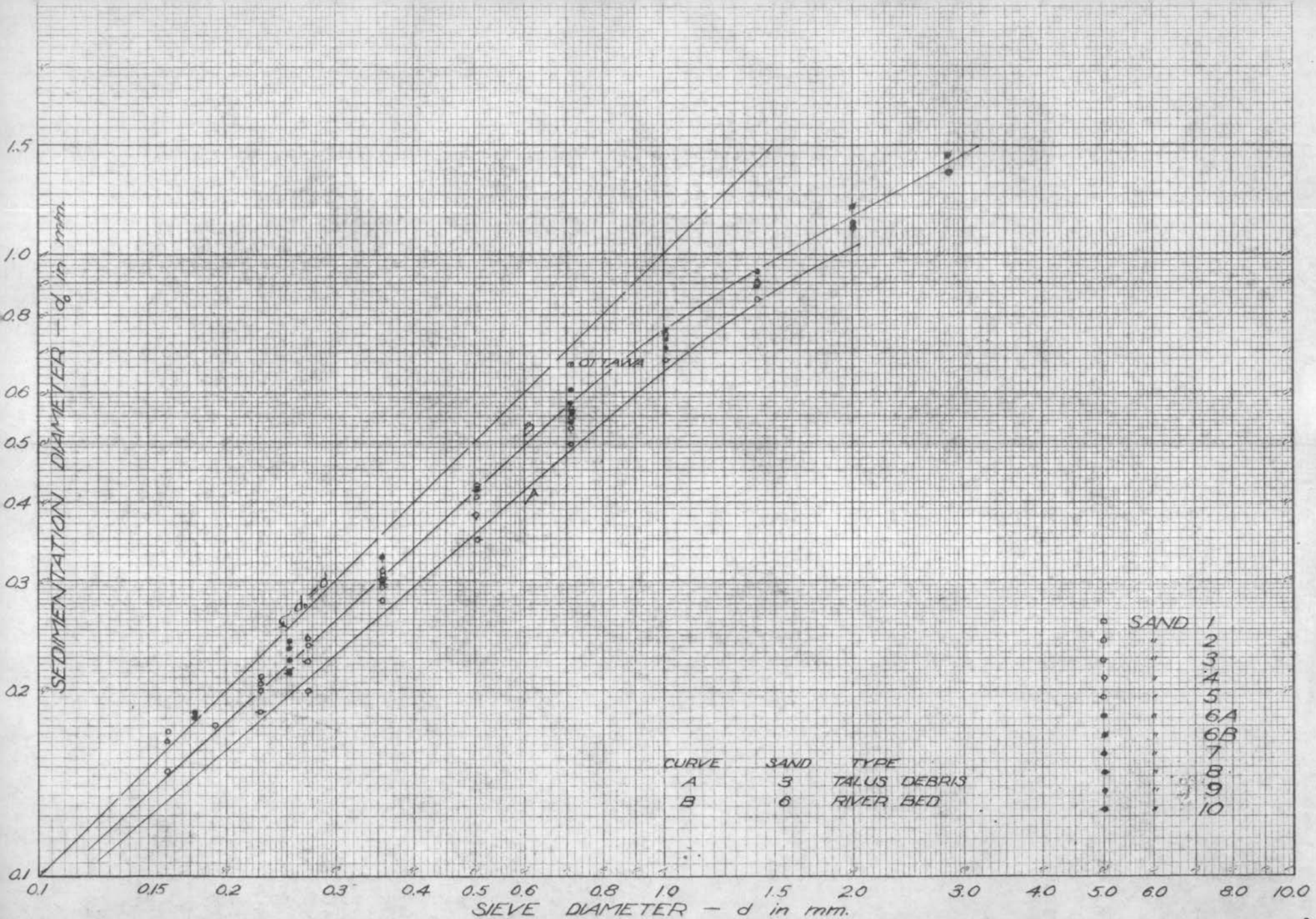


FIG. 3. VARIATION OF SEDIMENTATION DIAMETER WITH SIEVE DIAMETER



The experimental error appears sufficiently small for the purpose of this detailed comparison of the two diameters.

The procedure for using this data in estimating the mean sedimentation diameter and fall velocity of a sand when the mean sieve diameter and the degree of sphericity relative to the sands of this study are known will be briefly outlined. Either Figure 2 or 3 can be used in estimating the mean sedimentation diameter. The position of the  $d_0$  versus  $d$  curve for the particular sand must be estimated from the curves and data shown. Comparison of the photographs of Appendix C should help in this estimation. If the particle density is practically that of quartz, the mean fall velocity in centimeters per second for any temperature can be obtained with the estimated sedimentation diameter and available curves (6:41) for the terminal fall velocity of quartz spheres in water.

If the particle density differs appreciably from that of quartz, Figure 1 must be used. When the parameters

$$C_D = 4/3 \frac{(\rho_s - \rho_f) g d_n}{v_0^2 \rho_f} = \frac{F}{A \rho_f v_0^2 / 2}$$

$$\text{and } R = \frac{\rho_f v_0 d_n}{\mu} = \frac{v_0 d_n}{\nu}$$

are combined to eliminate  $v_0$ , the result,

$$C_D = 4/3 \frac{1}{R^2} \frac{\rho_f (\rho_s - \rho_f) g d_n^3}{\mu^2} = \frac{1}{R^2} \frac{2 F d_n^2}{A \rho_f \nu^2} = \frac{1}{R^2} \frac{8}{\pi} \frac{F}{\rho_f \nu^2}$$

$$\text{or } \log C_D = -2 \log R + \log \left( \frac{8}{\pi} \frac{F}{\rho_f \nu^2} \right) \quad (8)$$

is the equation of the lines of constant nominal diameter or constant resistance force. The intercept term on the right is calculated using the correct value of particle density ( $\beta$ ) and assuming the mean sieve diameter ( $d$ ) equal to the mean nominal diameter ( $d_0$ ). The position of the resistance curve for the particular sand is estimated from the curves and data shown. The intersection of the line of constant resistance force with the resistance curve yields  $R$  and  $C_D$  values, from either of which the terminal uniform settling velocity ( $v_0$ ) is determined. A superimposed scale of constant resistance force lines on the  $C_D$  versus  $R$  graph, as presented by Rouse (4, Fig. 125) is of considerable assistance in this problem.

Chapter V  
CONCLUSIONS

A detailed comparison of the sedimentation diameter ( $d_0$ ) and the sieve diameter ( $d$ ) for the range of sediment particle sizes 0.15 to 1.65 millimeters (10 to 100 meshes to the inch, Tyler Standard Screen Scale) and for particle shapes ranging from a highly spherical dune sand to a highly angular talus debris sample has been completed in this study. A procedure for estimating the mean sedimentation diameter and the corresponding fall velocity in water at any temperature is included.

The general conclusions of the study can be summarized as follows:

1. The family of resistance curves for sands of different average degrees of sphericity are asymptotic to the resistance curve for spheres in the direction of decreasing Reynolds number ( $R$ ). The difference between the two curves apparently becomes negligible when Stokes range is reached (about  $R = 0.1$ ). The flattening of the curves at a nominal diameter of about 1.5 millimeters indicates that this is about the size at which

viscous effects become secondary and the drag coefficient becomes independent of Reynolds number for the shape range of natural sands.

2. The points plotted on the  $C_D$  versus  $R$  graph, assuming the sieve diameter practically equal to the nominal diameter, scatter less from the lines of the assumed nominal diameters as the nominal diameters increase. Since the scatter is primarily a function of the sphericity of the particles, this study confirms the investigations of others showing that the sphericity of sand particles generally increases with size. Examination of the magnified photographs of Appendix C also confirms this observation.

3. The family of  $d_o$  versus  $d$  curves for sands is asymptotic to the  $d_o = d$  line in the direction of the origin. For practical purposes the difference between the two values becomes negligible for all sands at about  $d = 0.05$  millimeters. This confirms this value as the diameter of the coarsest particle for which the fall velocity in water at normal temperatures can be calculated by Stokes equation (based on viscous resistance only).

4. The  $d_o/d$  ratio decreases consistently in all sands from practically unity at  $d = 0.05$

millimeters to about 0.50 at  $d = 2.84$  millimeters (the average  $d$  for the 6 to 8 mesh fraction, Tyler Standard Screen Scale).

5. The  $d_0$  values for the most angular sand studied (talus debris, Sample 3) varied from 10% to 20% smaller than the  $d_0$  values of the corresponding fractions of the most spherical of the dune and river bed sands studied.

APPENDIX

## APPENDIX TABLE OF CONTENTS

Appendix	Page
A EXPERIMENTAL DATA, . . . . .	40
B CUMULATIVE CURVES OF MECHANICAL AND HYDRAULIC ANALYSES. . . . .	53
C ENLARGED PHOTOGRAPHS OF SANDS STUDIED . . . . .	64
D DEFINITIONS. . . . .	75
E NOTATION . . . . .	78

## Appendix A.--EXPERIMENTAL DATA

SIEVE ANALYSIS				HYDRAULIC ANALYSIS					
Tyler Mesh	Opening $\frac{d}{\text{mm.}}$	Wt. Ret. grams	Percent Finer	Mean Vel. $\bar{V}_0$ cm./sec.	Stand. Dev. $\sigma_{\bar{V}}$ cm./sec.	Temp. °F.	Viscosity $\mu$ dyne-sec/cm <sup>2</sup>	Density $\rho_f$ gm./cc.	Solid D. $\rho_s$ gm./cc.
10	1.651	Removed	100.0						
14	1.168 (1.001)	45.0	91.1 (82.6)	11.62	1.51	73.8	.00929	.9975	2.595
20	.834 (.712)	85.4	74.0 (62.4)	8.81	0.78	74.5	.00922	.9974	2.597
28	.589 (.503)	115.6	50.8 (39.3)	6.54	0.73	75.0	.00916	.9974	2.601
35	.417 (.356)	114.6	27.8 (20.4)	4.72	0.61	70.6	.00968	.9979	2.622
48	.295 (.271)	74.2	12.9 (10.7)	3.18	0.37	71.3	.00959	.9979	2.623
60	.246 (.227)	21.7	8.5 (7.2)	2.74	0.33	73.1	.00937	.9976	2.612
65	.208	12.9	5.9						
80	.175 (.161)	0.2	5.9 (4.7)	2.09	0.25	73.9	.00928	.9975	2.660
100	.147	12.2	3.5						
	Smaller	17.4							
	Total	499.2							

SAMPLE NUMBER 1

Source: Cache la Poudre River, Fort Collins, Colorado

SIEVE ANALYSIS				HYDRAULIC ANALYSIS					
Tyler Mesh	Opening $\frac{d}{\text{mm.}}$	Wt. Ret. grams	Percent Finer	Mean Vel. $\bar{V}_{50}$ cm./sec.	Stand. Dev. $\sigma_{\bar{v}}$ cm./sec.	Temp. °F.	Viscosity $\mu$ dyne-sec/cm <sup>2</sup>	Density $\rho_f$ gm./cc.	Solid D. $\rho_s$ gm./cc.
10	1.651 (1.410)	Removed	100.0 (95.0)	13.95	1.65	74.5	.00922	.9974	2.585
14	1.168 (1.001)	50.2	89.9 (83.0)	11.56	1.55	74.5	.00922	.9974	2.585
20	.834 (.712)	68.0	76.2 (68.8)	8.45	1.14	74.5	.00922	.9974	2.585
28	.589 (.503)	73.0	61.5 (51.8)	6.21	0.58	74.3	.00924	.9975	2.594
35	.417 (.356)	95.9	42.2 (30.1)	4.51	0.51	74.2	.00925	.9975	2.606
48	.295 (.270)	120.5	18.0 (14.0)	3.38	0.40	75.1	.00915	.9974	2.620
60	.246 (.227)	39.5	10.1 (7.6)	2.70	0.30	75.4	.00911	.9973	2.620
65	.208	24.5	5.2						
80	.175 (.161)	4.7	4.2 (2.8)	1.98	0.29	76.0	.00905	.9972	2.622
100	.147	14.6	1.3						
	Smaller	6.3							
	Total	497.2							

SAMPLE NUMBER 2

Source: Michigan River, Camp Pennock, Colorado

SIEVE ANALYSIS				HYDRAULIC ANALYSIS					
Tyler Mesh	Opening $\frac{d}{\text{mm.}}$	Wt. Ret. grams	Percent Finer	Mean Vel. $\bar{V}_0$ cm./sec.	Stand. Dev. $\sigma_0$ cm./sec.	Temp. °F.	Viscosity $\mu$ dyne-sec/cm <sup>2</sup>	Density $\rho_f$ gm./cc.	Solid D. $\rho_s$ gm./cc.
10	1.651 (1.410)	Removed	100.0 (92.0)	12.36	1.92	73.5	.00933	.9976	2.457
14	1.168 (1.001)	80.1	83.9 (71.0)	9.84	1.32	73.2	.00936	.9976	2.430
20	.834 (.712)	128.2	58.1 (47.3)	7.76	0.95	73.2	.00936	.9976	2.418
28	.589 (.503)	107.2	36.5 (28.3)	4.66	0.60	74.1	.00926	.9975	2.389
35	.417 (.356)	81.4	20.1 (14.4)	3.71	0.50	74.4	.00923	.9975	2.379
48	.295 (.270)	56.9	8.7 (7.4)	2.79	0.39	75.2	.00913	.9974	2.330
60	.246 (.227)	12.6	6.2 (5.3)	1.98	0.26	76.2	.00901	.9972	2.319
65	.208	9.0	4.4						
80	.175	0.3	4.3						
100	.147	8.0	2.7						
	Smaller	13.5							
	Total	497.2							

SAMPLE NUMBER 3

Source: Talus slide, Verdi, Nevada

SIEVE ANALYSIS				HYDRAULIC ANALYSIS					
Tyler Mesh	Opening $\frac{d}{\text{mm.}}$	Wt. Ret. grams	Percent Finer	Mean Vel. $\bar{V}_0$ cm./sec.	Stand. Dev. $\sigma_{V_0}$ cm./sec.	Temp. °F.	Viscosity $\mu$ dyne-sec/cm <sup>2</sup>	Density $\rho_f$ gm./cc.	Solid D. $\rho_s$ gm./cc.
10	1.651	None							
14	1.168	Neglig.	100.0						
20	.834 (.712)	1.9	99.6 (98.2)	7.80	1.03	75.2	.00914	.9974	2.496
28	.589 (.503)	13.5	96.9 (91.0)	5.81	0.74	75.3	.00913	.9973	2.602
35	.417 (.356)	59.3	85.0 (72.2)	4.91	0.62	75.3	.00912	.9973	2.629
48	.295 (.271)	128.4	59.3 (55.0)	3.32	0.31	76.5	.00899	.9972	2.638
60	.246 (.227)	43.6	50.6 (45.5)	2.74	0.31	79.2	.00870	.9968	2.678
65	.208 (.192)	50.8	40.4 (38.8)	2.23	0.24	79.8	.00864	.9967	2.621
80	.175 (.161)	16.2	37.1 (31.4)	1.80	0.25	80.5	.00855	.9966	2.686
100	.147	57.1	25.7						
	Smaller	128.3							
	Total	499.1							

SAMPLE NUMBER 4

Source: Dunes, Fernley, Nevada

SIEVE ANALYSIS				HYDRAULIC ANALYSIS					
Tyler Mesh	Opening $d$ mm.	Wt. Ret. grams	Percent Finer	Mean Vel. $\bar{V}_0$ cm./sec.	Stand. Dev. $\sigma_{\bar{V}_0}$ cm./sec.	Temp. °F.	Viscosity $\mu$ dyne-sec/cm <sup>2</sup>	Density $\rho_f$ gm./cc.	Solid D. $\rho_s$ gm./cc.
10	1.651	Neglig.	100.0						
14	1.168	1.7	99.7						
20	.834	8.3	98.0						
	(.712)		(95.1)	7.50	1.23	78.9	.00874	.9968	2.479
28	.589	28.8	92.2						
	(.503)		(84.2)	5.74	0.66	80.3	.00857	.9966	2.530
35	.417	80.1	76.1						
	(.356)		(58.8)	4.03	0.54	80.6	.00854	.9966	2.569
48	.295	171.8	41.5						
	(.270)		(36.4)	3.04	0.31	76.5	.00899	.9972	2.619
60	.246	50.4	31.4						
	(.227)		(26.3)	2.41	0.21	78.1	.00882	.9970	2.649
65	.208	50.9	21.2						
	(.192)		(19.6)	2.17	0.19	79.5	.00867	.9968	2.601
80	.175	16.1	18.0						
100	.147	36.0	10.7						
	Smaller	53.4							
	Total	497.5							

SAMPLE NUMBER 5

Source: Truckee River, Truckee, California

SIEVE ANALYSIS				HYDRAULIC ANALYSIS					
Tyler Mesh	Opening $\frac{d}{\text{mm.}}$	Wt. Ret. grams	Percent Finer	Mean Vel. $\bar{V}_0$ cm./sec.	Stand. Dev. $\sigma_{\bar{V}_0}$ cm./sec.	Temp. °F.	Viscosity $\mu$ dyne-sec/cm <sup>2</sup>	Density $\rho_f$ gm./cc.	Solid D. $\rho_s$ gm./cc.
6	3.327 (2.844)	Removed	100.00 (98.30)	20.51	3.37	77.8	.00885	.9970	2.542
8	2.362 (2.006)	17.0	96.59 (90.36)	17.17	1.76	77.6	.00887	.9970	2.529
10	1.651 (1.410)	62.1	84.14 (72.62)	14.06	1.91	77.5	.00889	.9970	2.569
14	1.168 (1.001)	114.9	61.09 (48.61)	11.52	1.38	77.0	.00894	.9971	2.575
20	.834 (.712)	124.4	36.13 (29.46)	9.41	0.91	77.0	.00894	.9971	2.572
28	.589 (.503)	66.5	22.79 (18.34)	6.51	0.70	77.1	.00892	.9971	2.581
35	.417 (.356)	44.4	13.89 (10.48)	4.22	0.54	76.5	.00899	.9972	2.587
48	.295 (.252)	34.0	7.07 (5.14)	2.98	0.43	77.5	.00888	.9970	2.541
65	.208	19.2	3.22						
100	.147	8.4	1.54						
	Smaller	7.7							
	Total	498.6							

SAMPLE NUMBER 6

First Analysis

Source: South Fork Yuba River, Cisco, California

SIEVE ANALYSIS				HYDRAULIC ANALYSIS					
Tyler Mesh	Opening $\frac{d}{\text{mm.}}$	Wt. Ret. grams	Percent Finer	Mean Vel. $\bar{V}_0$ cm./sec.	Stand. Dev. $\sigma_{\bar{V}_0}$ cm./sec.	Temp. °F.	Viscosity $\mu$ dyne-sec/cm <sup>2</sup>	Density $\rho_f$ gm./cc.	Solid D. $\rho_s$ gm./cc.
6	3.327 (2.844)	Removed	100.00 (98.26)	21.27	2.45	77.8	.00884	.9970	2.493
8	2.362 (2.006)	17.1	96.52 (90.88)	18.31	2.34	78.4	.00878	.9969	2.532
10	1.651 (1.410)	55.5	85.24 (73.00)	14.19	1.80	79.0	.00872	.9968	2.566
14	1.168 (1.001)	120.5	60.75 (48.66)	12.14	1.45	81.6	.00844	.9964	2.564
20	.834 (.712)	119.0	36.57 (29.82)	8.94	0.82	82.2	.00838	.9964	2.589
28	.589 (.503)	66.4	23.07 (18.56)	6.70	0.80	83.0	.00831	.9962	2.599
35	.417 (.356)	44.4	14.05 (10.42)	4.39	0.64	77.0	.00894	.9971	2.608
48	.295 (.252)	35.7	6.79 (4.97)	2.85	0.38	78.1	.00882	.9970	2.585
65	.208	17.9	3.15						
100	.147	7.5	1.63						
	Smaller	8.0							
	Total	492.0							

SAMPLE NUMBER 6

Second Analysis

Source: South Fork Yuba River, Cisco, California

SIEVE ANALYSIS				HYDRAULIC ANALYSIS					
Tyler Mesh	Opening $\frac{d}{\text{mm.}}$	Wt. Ret. grams	Percent Finer	Mean Vel. $\bar{V}_0$ cm./sec.	Stand. Dev. $\sigma_{V_0}$ cm./sec.	Temp. °F.	Viscosity $\mu$ dyne-sec/cm <sup>2</sup>	Density $\rho_p$ gm./cc.	Solid D. $\rho_s$ gm./cc.
6	3.327	Neglig.	100.0						
8	2.362	0.3	99.9						
10	1.651	0.7	99.8						
14	1.168	7.6	98.3						
	(1.001)		(94.2)	11.21	1.42	74.7	.00920	.9974	2.619
20	.834	40.9	90.1						
	(.712)		(74.6)	8.61	0.84	76.0	.00905	.9973	2.629
28	.589	153.4	59.2						
	(.503)		(37.4)	6.68	0.75	76.8	.00896	.9971	2.672
35	.417	216.9	15.6						
	(.356)		(8.7)	5.04	0.55	79.2	.00870	.9968	2.662
48	.295	68.5	1.8						
65	.208	7.9	0.2						
100	.147	0.6	0.1						
	Smaller	0.4							
	Total	497.2							

SAMPLE NUMBER 7

Source: Putah Creek, Davis, California

SIEVE ANALYSIS				HYDRAULIC ANALYSIS					
Tyler Mesh	Opening $\frac{d}{\text{mm.}}$	Wt. Ret. grams	Percent Finer	Mean Vel. $\bar{V}_0$ cm./sec.	Stand. Dev. $\sigma_{\bar{V}_0}$ cm./sec.	Temp. °F.	Viscosity $\mu$ dyne-sec/cm <sup>2</sup>	Density $\rho_f$ gm./cc.	Solid D. $\rho_s$ gm./cc.
10	1.651	None	100.00						
14	1.168	0.2	99.97						
20	.834	0.5	99.87						
28	.589	1.3	99.61						
	(.503)		(98.84)	6.61	0.89	79.0	.00872	.9968	2.631
35	.417	7.7	98.07						
	(.356)		(65.05)	4.84	0.70	80.5	.00854	.9966	2.808
48	.295	331.0	32.03						
	(.252)		(19.94)	3.58	0.39	80.7	.00853	.9966	2.794
65	.208	121.2	7.85						
	(.178)		(4.64)	2.51	0.38	79.1	.00871	.9968	2.772
100	.147	32.1	1.44						
	Smaller	7.2							
	Total	501.2							

SAMPLE NUMBER 8

Source: Dunes near Great Salt Lake, Utah

SIEVE ANALYSIS				HYDRAULIC ANALYSIS					
Tyler Mesh	Opening $\frac{d}{\text{mm.}}$	Wt. Ret. grams	Percent Finer	Mean Vel. $\bar{V}_0$ cm./sec.	Stand. Dev. $\sigma_{\bar{V}_0}$ cm./sec.	Temp. °F.	Viscosity $\mu$ dyne-sec/cm <sup>2</sup>	Density $\rho_f$ gm./cc.	Solid D. $\rho_s$ gm./cc.
6	3.327	Neglig.	100.0						
8	2.362 (1.410)	4.1	99.18 (97.90)	17.02	2.09	82.6	.00834	.9963	2.512
10	1.651 (1.410)	12.8	96.61 (92.20)	14.26	1.70	78.5	.00877	.9969	2.588
14	1.168 (1.001)	44.1	87.78 (78.54)	11.57	1.38	79.2	.00870	.9968	2.653
20	.834 (.712)	92.2	69.30 (56.16)	9.23	0.94	79.6	.00866	.9967	2.594
28	.589 (.503)	131.1	43.02 (30.42)	6.67	0.90	81.2	.00848	.9965	2.604
35	.417 (.356)	125.7	17.82 (11.92)	4.52	0.54	78.2	.00881	.9969	2.592
48	.295 (.252)	58.9	6.01 (3.82)	3.35	0.42	78.9	.00874	.9968	2.578
65	.208	21.9	1.62						
100	.147	6.1	0.40						
	Smaller	2.0							
	Total	498.9							
SAMPLE NUMBER 9									
Source: Beach, Grand Lake, Colorado									

SIEVE ANALYSIS				HYDRAULIC ANALYSIS					
Tyler Mesh	Opening $\frac{d}{\text{mm.}}$	Wt. Ret. grams	Percent Finer	Mean Vel. $\frac{V_0}{\text{cm./sec.}}$	Stand. Dev. $\frac{\sigma}{V_0}$ cm./sec.	Temp. °F.	Viscosity $\mu$ dyne-sec/cm <sup>2</sup>	Density $\rho_p$ gm./cc.	Solid D. $\rho_s$ gm./cc.
10	1.651 (1.410)	Removed	100.00 (94.46)	14.85	2.00	77.8	.00885	.9970	2.594
14	1.168 (1.001)	54.9	88.97 (79.82)	11.93	1.42	78.1	.00881	.9969	2.605
20	.834 (.712)	91.1	70.67 (61.22)	8.94	1.00	78.6	.00876	.9969	2.602
28	.589 (.503)	94.1	51.77 (41.58)	6.55	0.73	79.4	.00868	.9968	2.617
35	.417 (.356)	101.5	31.38 (22.88)	4.62	0.62	82.5	.00835	.9963	2.617
48	.295 (.252)	84.7	14.37 (10.52)	3.02	0.49	82.7	.00833	.9963	2.642
65	.208 (.178)	38.3	6.68 (5.18)	2.25	0.28	83.5	.00825	.9962	2.599
100	.147	14.9	3.69						
	Smaller	18.4							
	Total	497.9							

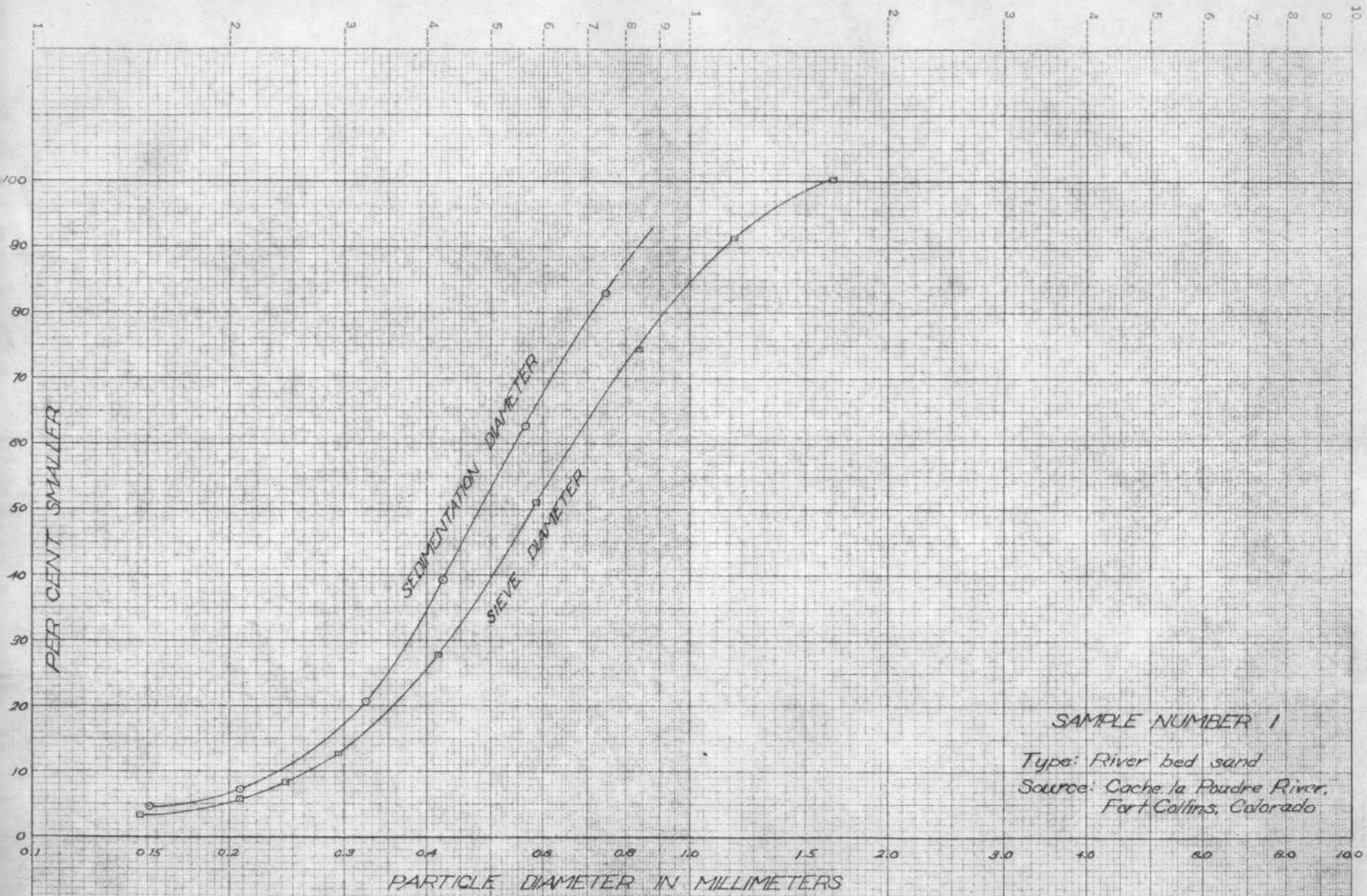
SAMPLE NUMBER 10

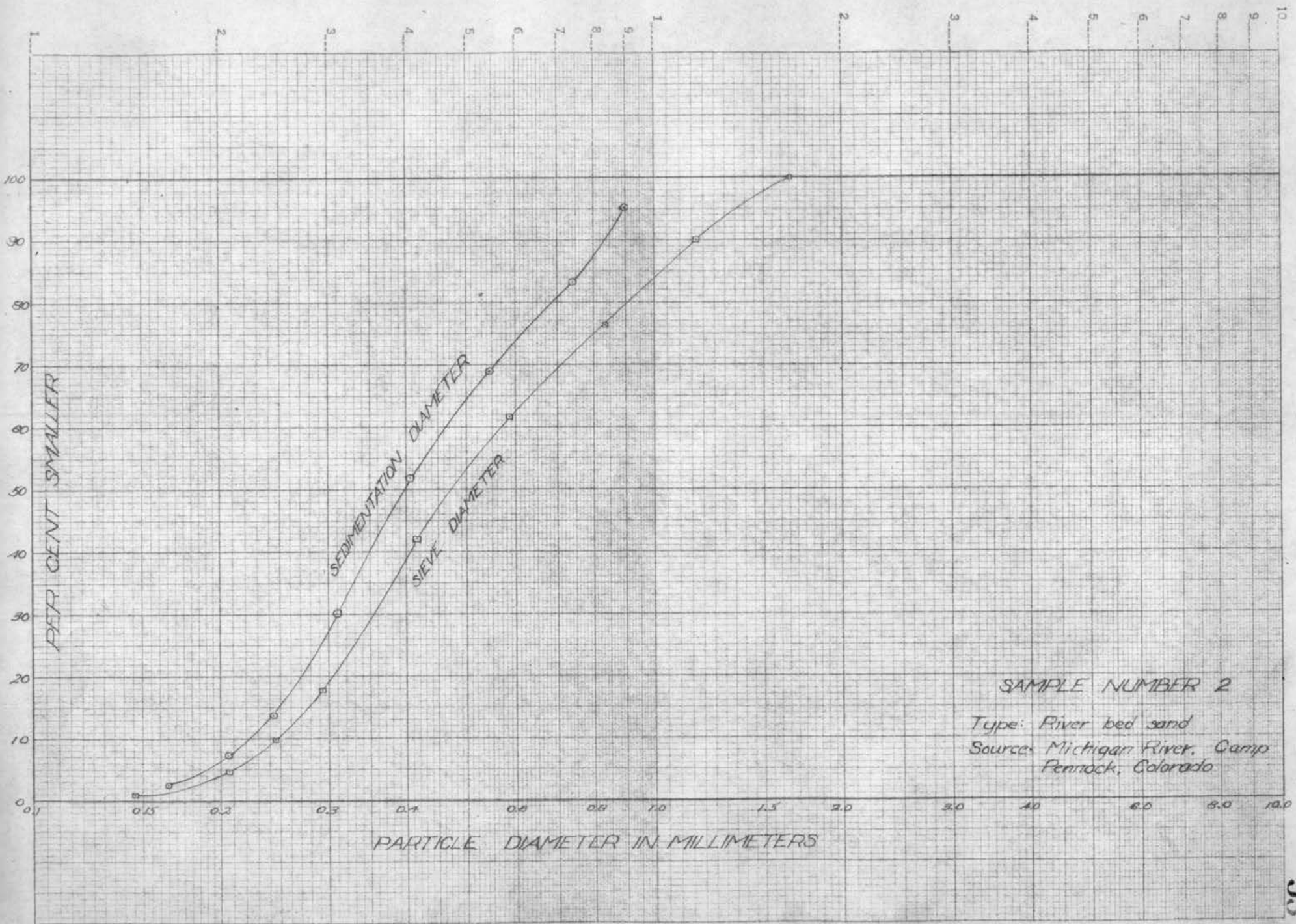
Source: Cache la Poudre River, Chambers Lake, Colorado

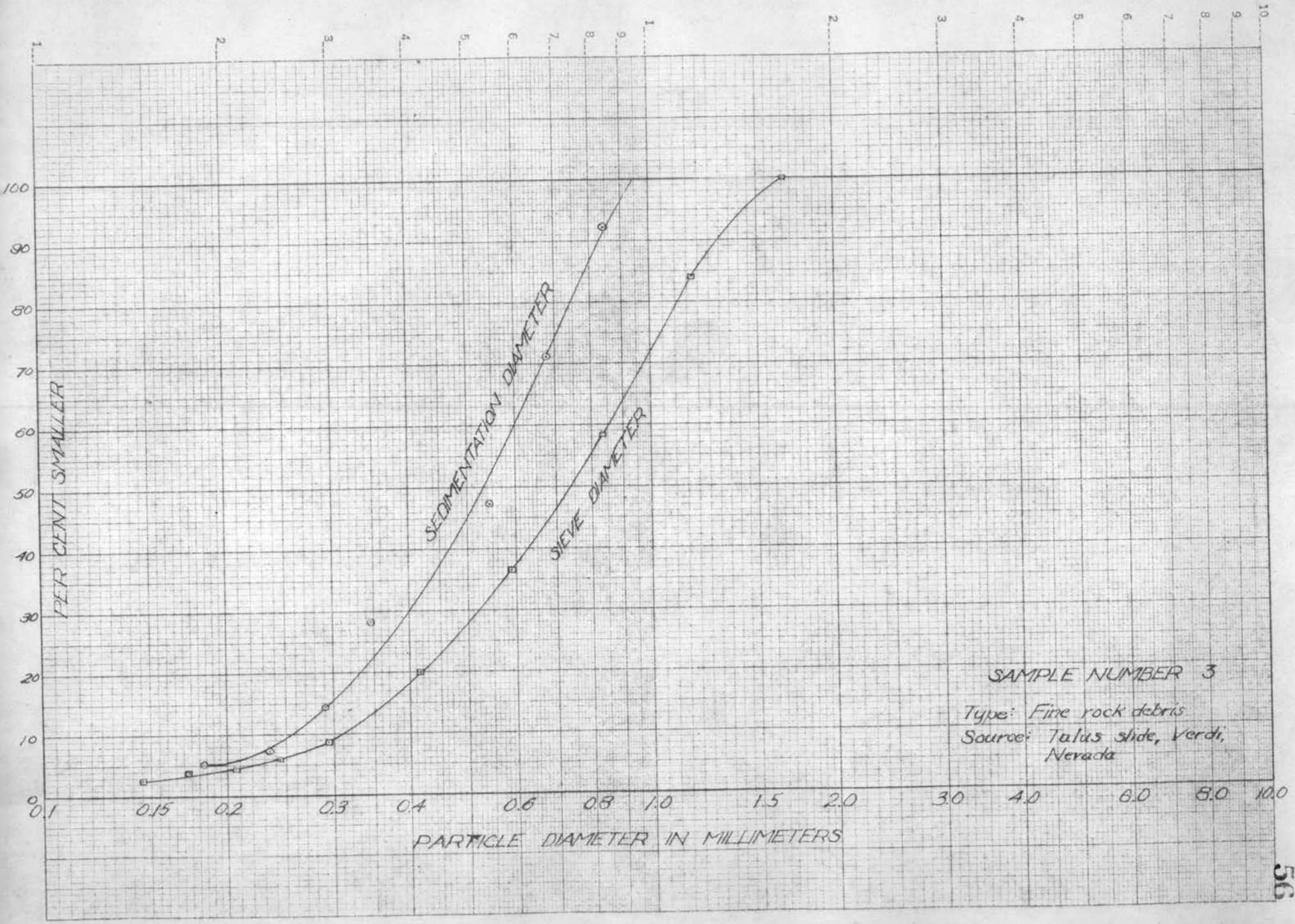
SIEVE ANALYSIS				HYDRAULIC ANALYSIS					
Tyler Mesh	Opening $\frac{d}{\text{mm.}}$	Wt. Ret. grams	Percent Finer	Mean Vel. $\frac{V}{\text{cm./sec.}}$	Stand. Dev. $\frac{\sigma}{\text{cm./sec.}}$	Temp. °F.	Viscosity $\mu$ dyne-sec/cm <sup>2</sup>	Density $\rho_f$ gm./cc.	Solid D. $\rho_s$ gm./cc.
14	1.168	Neglig.	100.0	10.58	0.55	76.1	.00904	.9972	2.617
20	0.834 (0.712)	6.0	98.8 (49.6)						
28	0.589	491.8	0.5						
35	0.417	2.5	0						
	Total	500.3							

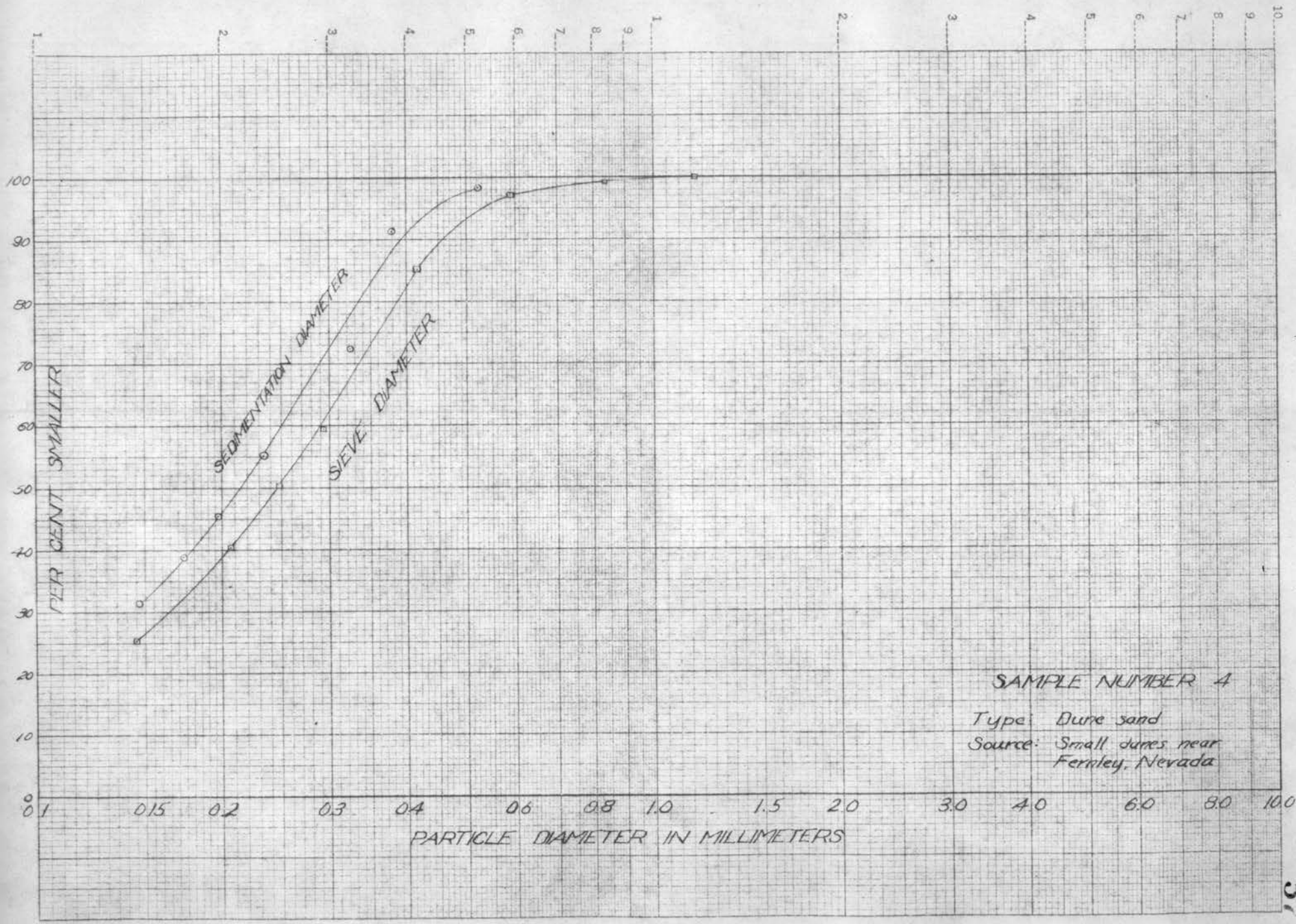
Standard Ottawa Sand

Appendix B.--CUMULATIVE CURVES  
OF MECHANICAL AND HYDRAULIC  
ANALYSES

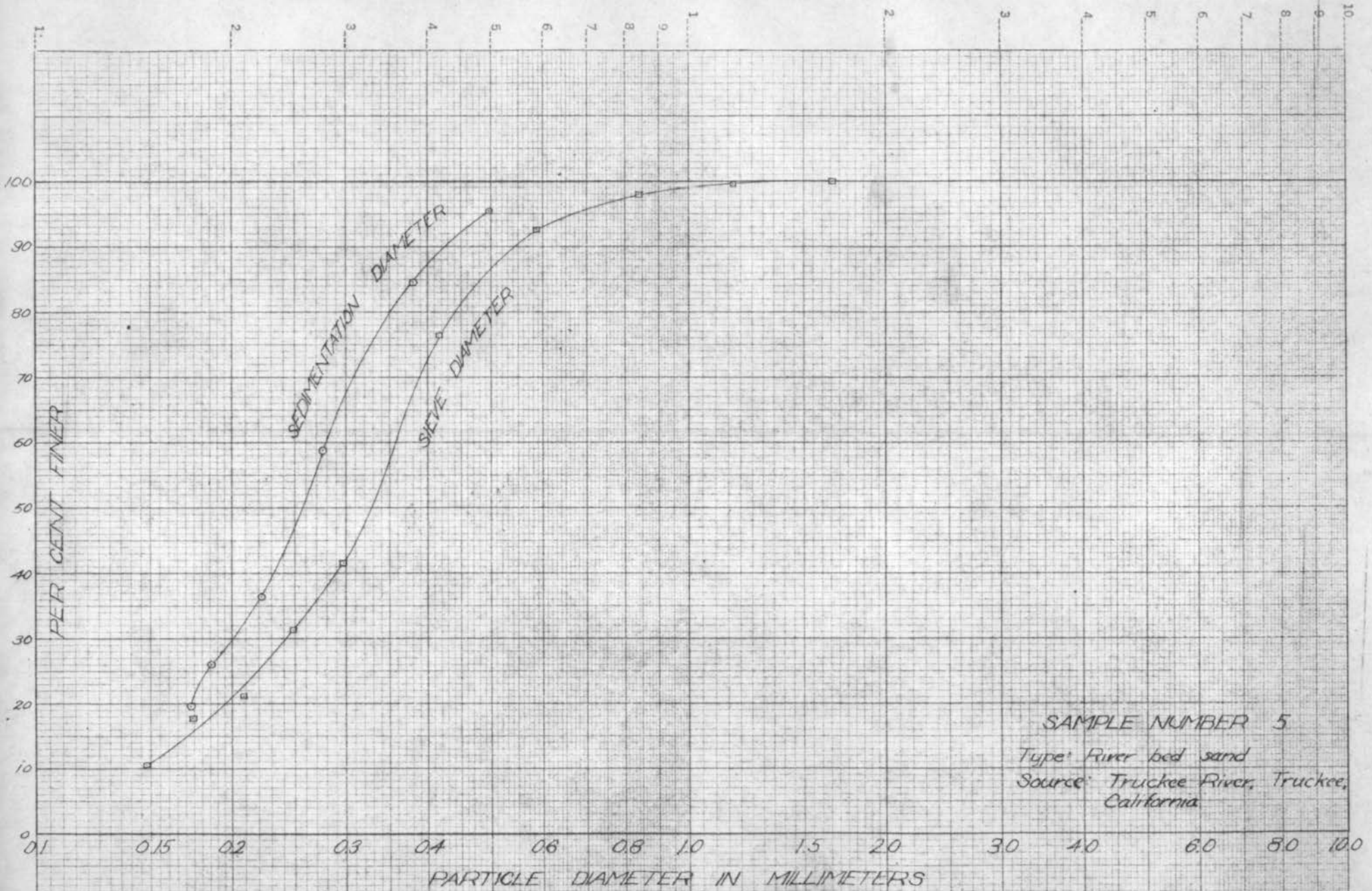




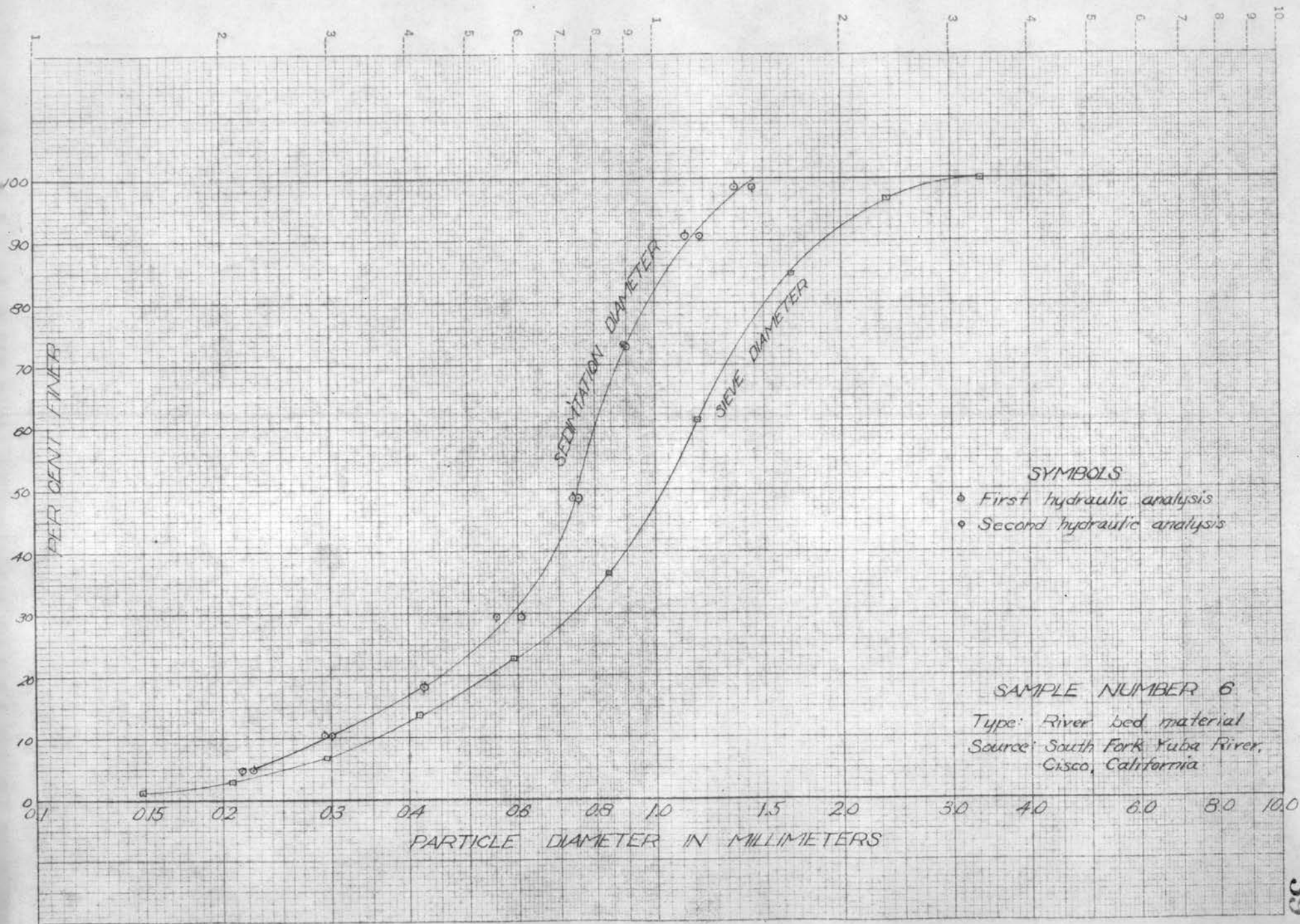


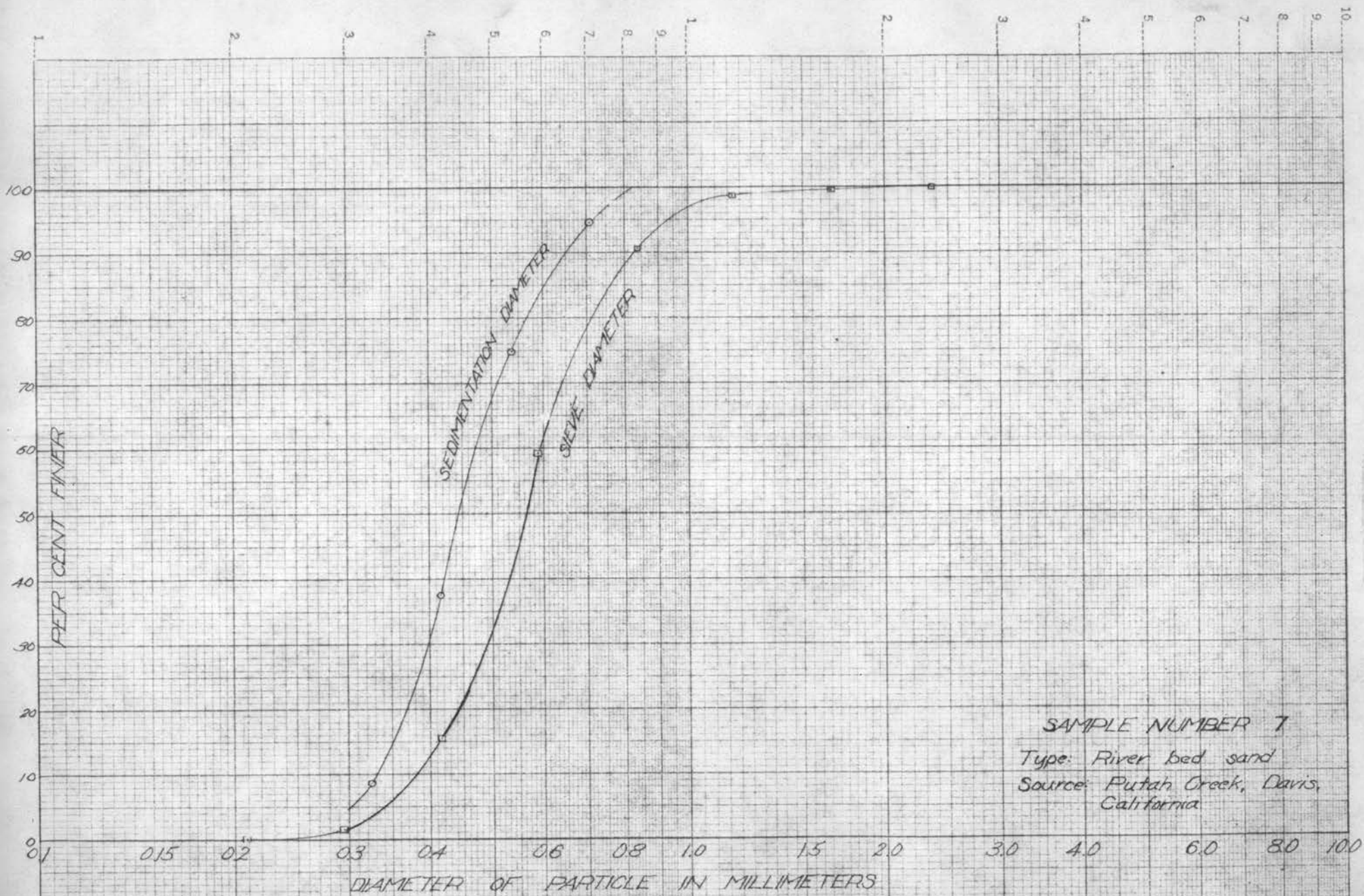


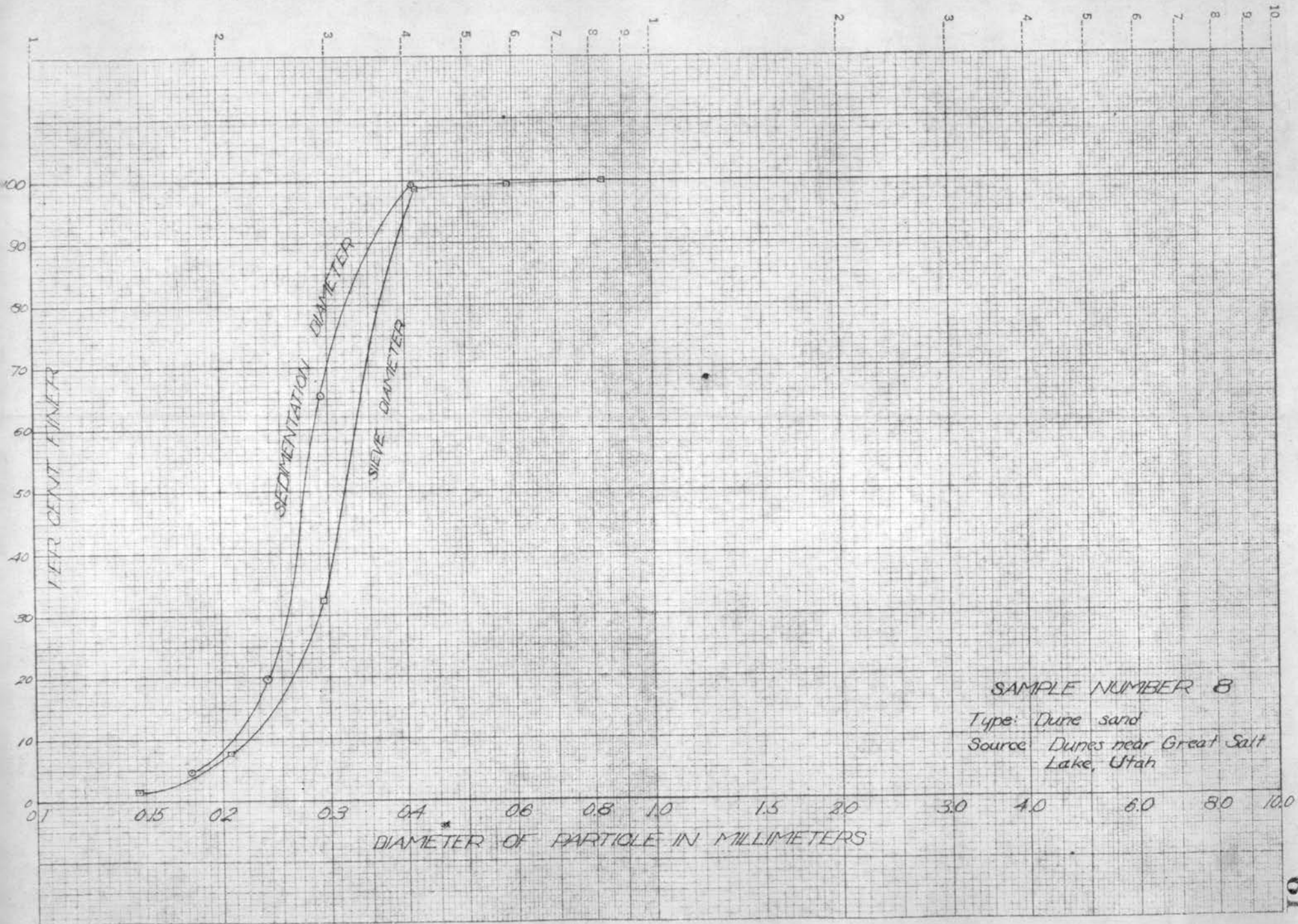
SAMPLE NUMBER 4  
Type: Pure sand  
Source: Small dunes near  
Fernley, Nevada



SAMPLE NUMBER 5  
Type: River bed sand  
Source: Truckee River, Truckee,  
California

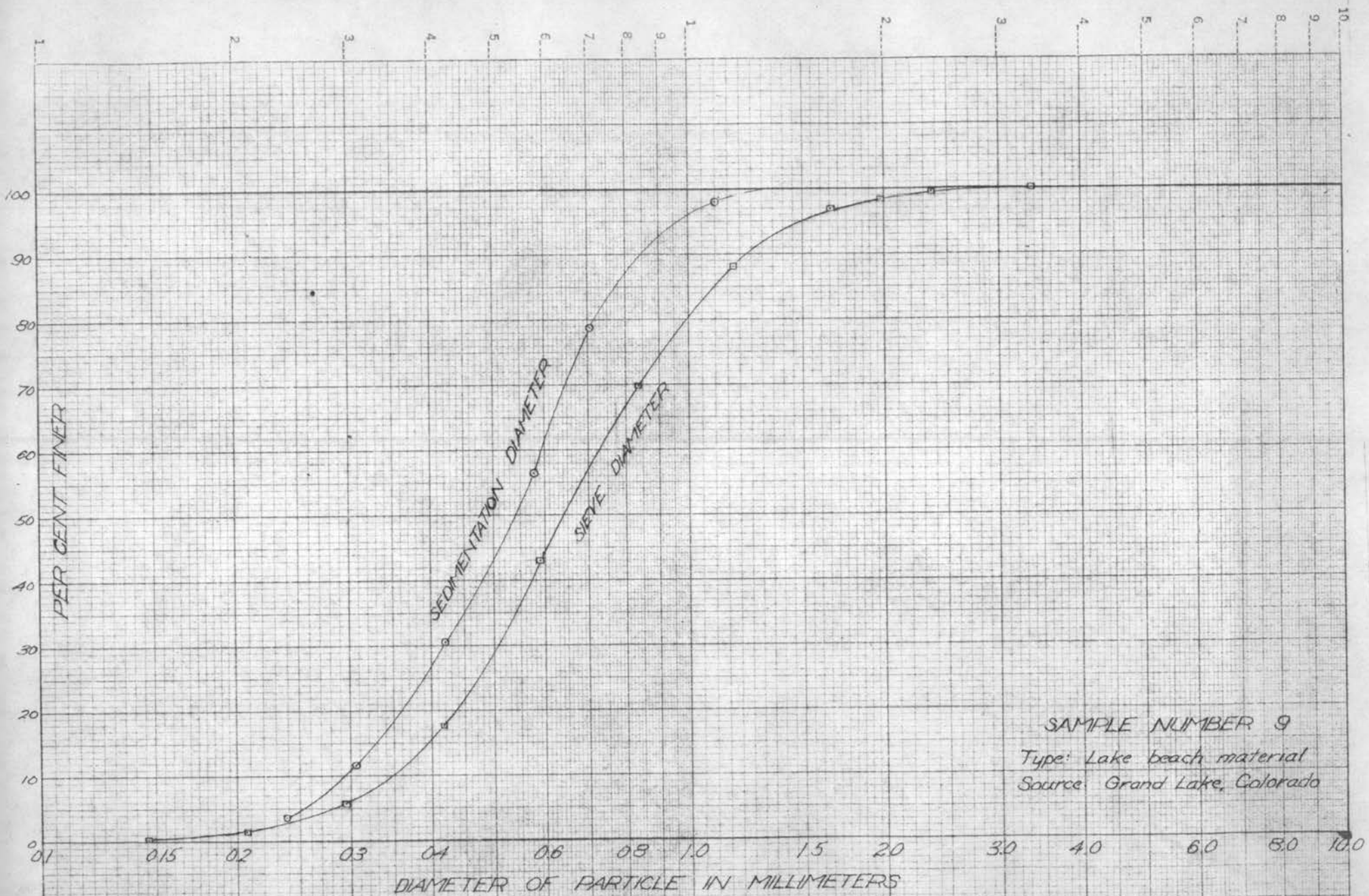


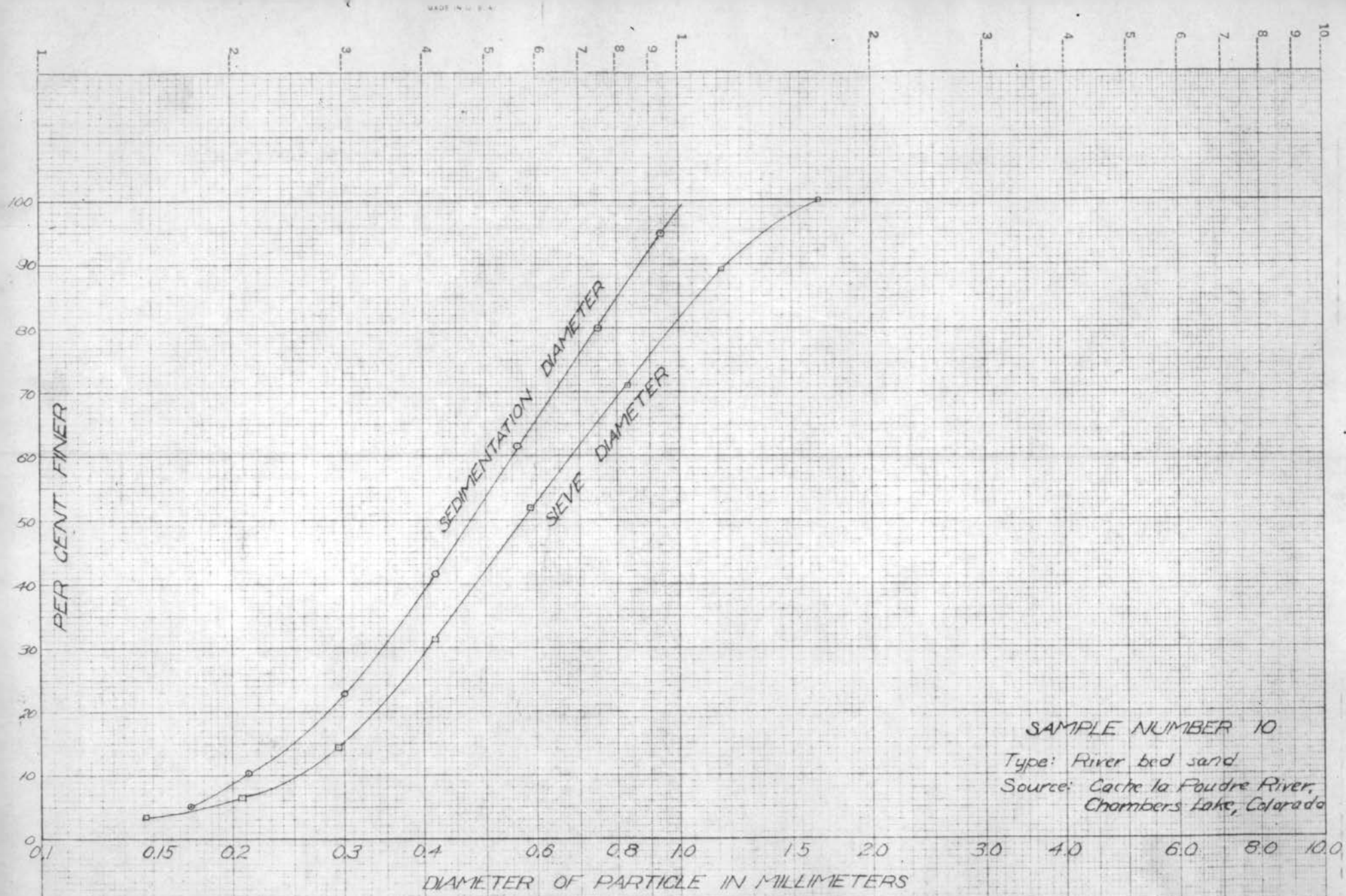




SAMPLE NUMBER 8

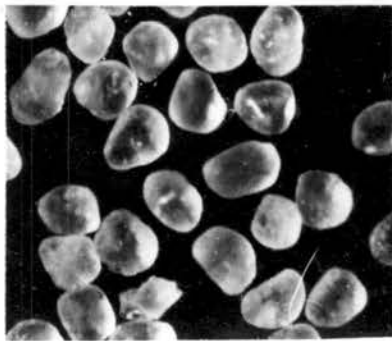
Type: Dune sand  
Source: Dunes near Great Salt Lake, Utah





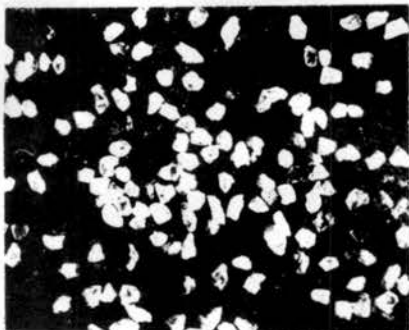
## APPENDIX C

## ENLARGED PHOTOGRAPHS OF PARTICLES

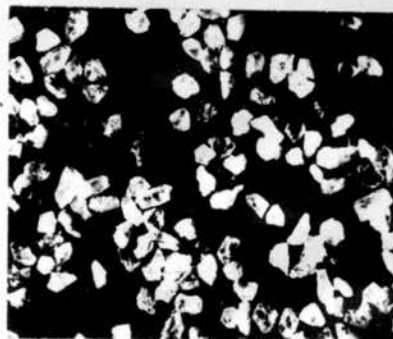


STANDARD OTTAWA SAND

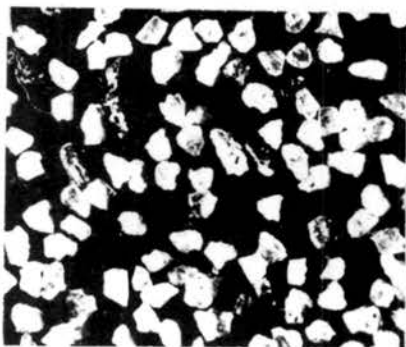
Tyler Sieves 28 - 20  
Average 0.712 mm.



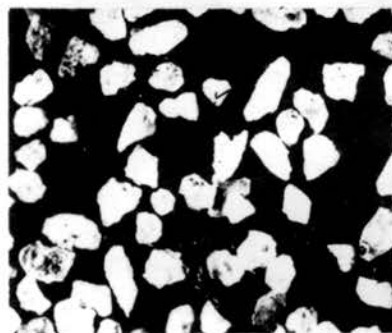
Tyler Sieves 100 - 80  
Average 0.161 mm.



Tyler Sieves 65 - 60  
Average 0.227 mm.



Tyler Sieves 60 - 48  
Average 0.271 mm.



Tyler Sieves 48 - 35  
Average 0.356 mm.



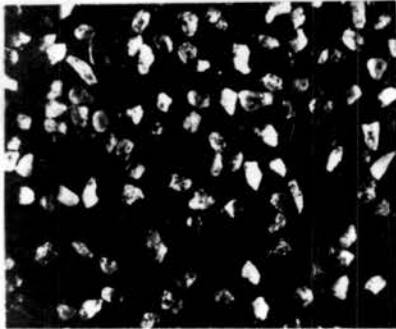
Tyler Sieves 35 - 28  
Average 0.503 mm.



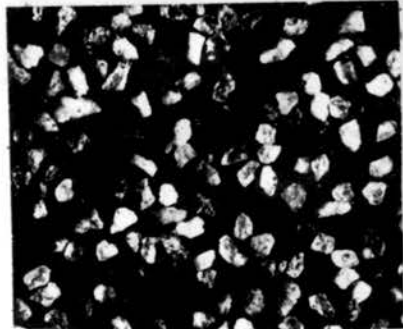
Tyler Sieves 28 - 20  
Average 0.712 mm.

SAND SAMPLE NUMBER 1  
Magnification 10 diameters

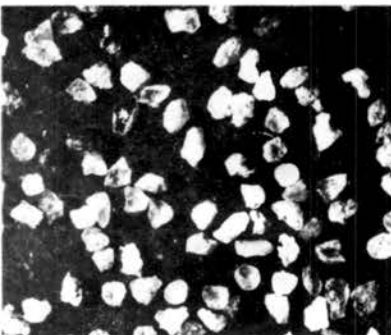
Type: River bed material  
Source: Cache la Poudre R., Fort Collins,  
Colorado



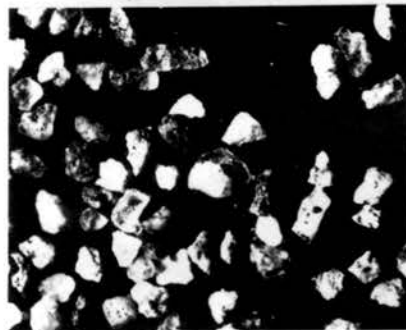
Tyler Sieves 80 - 65  
Average 0.192 mm.



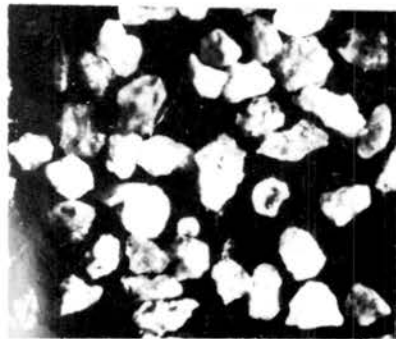
Tyler Sieves 65 - 60  
Average 0.227 mm.



Tyler Sieves 60 - 48  
Average 0.270 mm.



Tyler Sieves 48 - 35  
Average 0.356 mm.



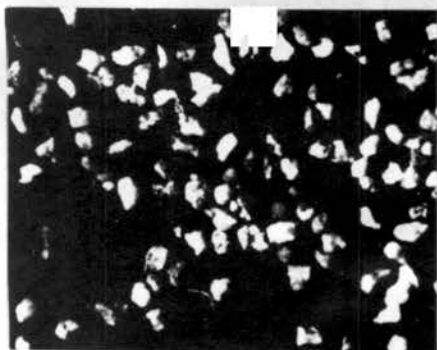
Tyler Sieves 35 - 28  
Average 0.503 mm.



Tyler Sieves 28 - 20  
Average 0.712 mm.

SAND SAMPLE NUMBER 2  
Magnification 10 diameters

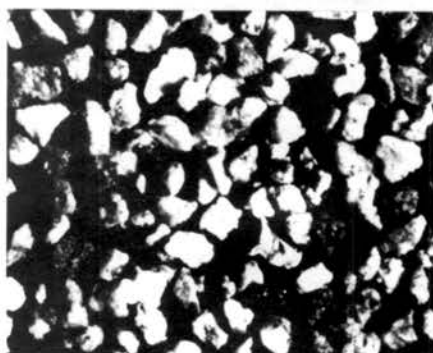
Type: River bed material  
Source: Michigan River, Camp Pennock,  
Colorado



Tyler Sieves 65 - 60  
Average 0.227 mm.



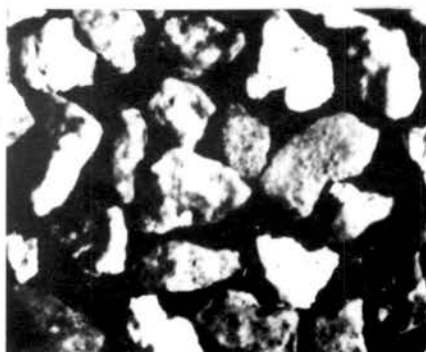
Tyler Sieves 60 - 48  
Average 0.270 mm.



Tyler Sieves 48 - 35  
Average 0.356 mm.



Tyler Sieves 35 - 28  
Average 0.503 mm.



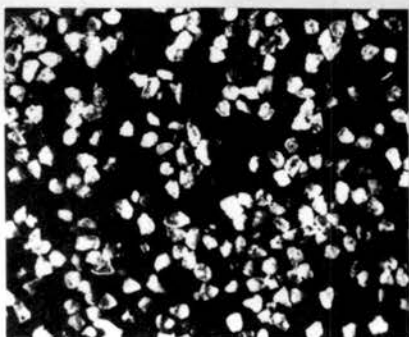
Tyler Sieves 28 - 20  
Average 0.712 mm.



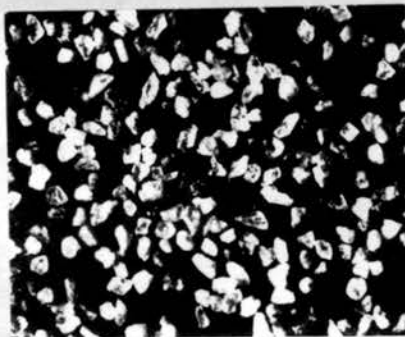
Tyler Sieves 14 - 10  
Average 1.410 mm.

SAND SAMPLE NUMBER 3  
Magnification 10 diameters

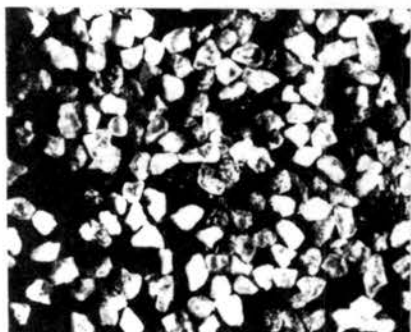
Type: Fine rock debris  
Source: Fresh talus slide, Verdi, Nevada



Tyler Sieves 80 - 65  
Average 0.192 mm.



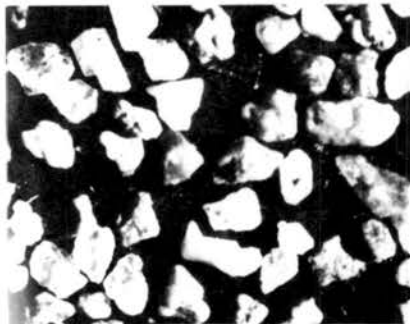
Tyler Sieves 65 - 60  
Average 0.227 mm.



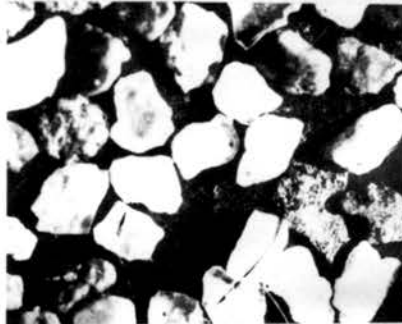
Tyler Sieves 60 - 48  
Average 0.270 mm.



Tyler Sieves 48 - 35  
Average 0.356 mm.



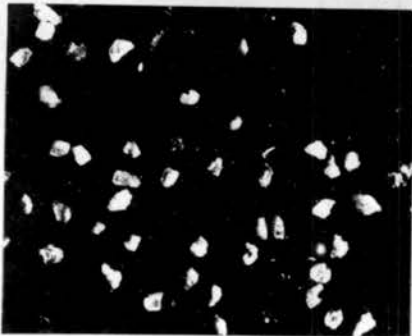
Tyler Sieves 35 - 28  
Average 0.503 mm.



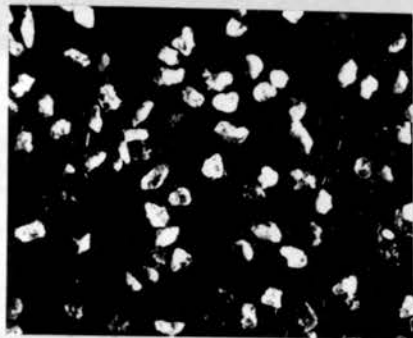
Tyler Sieves 28 - 20  
Average 0.712 mm.

SAND SAMPLE NUMBER 4  
Magnification 10 diameters

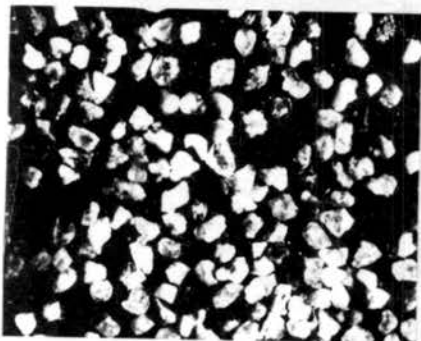
Type: Dune sand  
Source: Fernley, Nevada



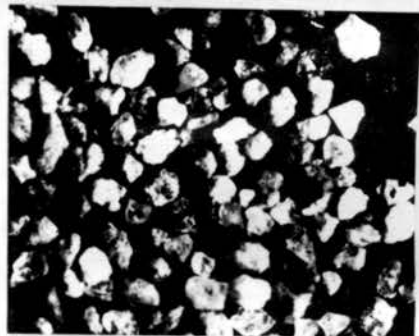
Tyler Sieves 80 - 65  
Average 0.192 mm.



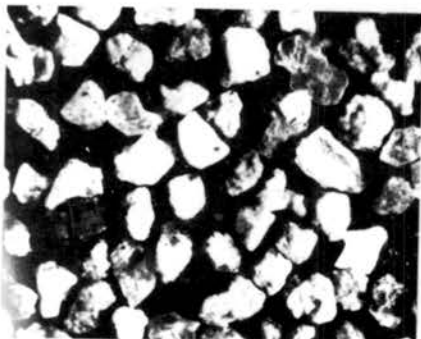
Tyler Sieves 65 - 60  
Average 0.227 mm.



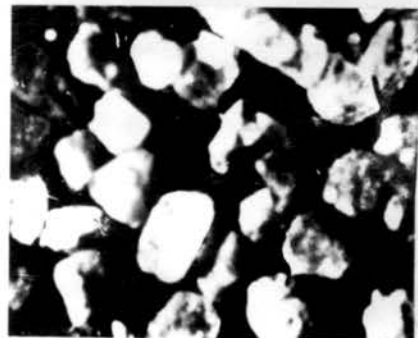
Tyler Sieves 60 - 48  
Average 0.270 mm.



Tyler Sieves 48 - 35  
Average 0.356 mm.



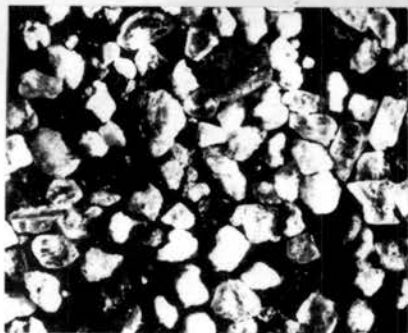
Tyler Sieves 35 - 28  
Average 0.503 mm.



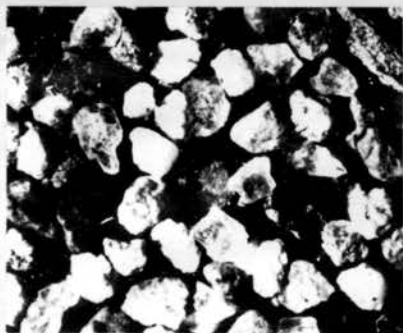
Tyler Sieves 28 - 20  
Average 0.712 mm.

SAND SAMPLE NUMBER 5  
Magnification 10 diameters

Type: River bed material  
Source: Truckee River, Truckee, California



Tyler Sieves 48 - 35  
Average 0.356 mm.



Tyler Sieves 35 - 28  
Average 0.503 mm.



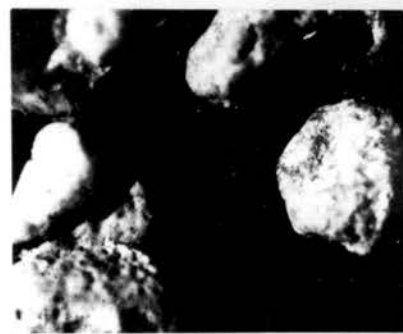
Tyler Sieves 28 - 20  
Average 0.712 mm.



Tyler Sieves 20 - 14  
Average 1.001 mm.



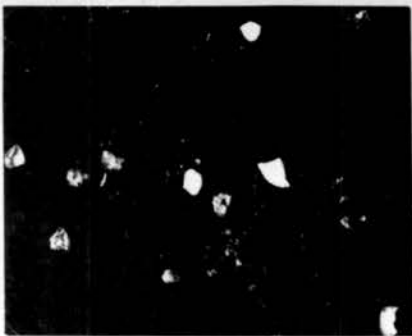
Tyler Sieves 14 - 10  
Average 1.410 mm.



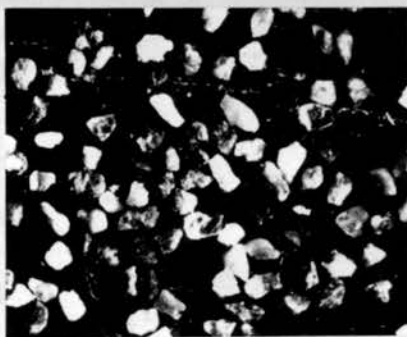
Tyler Sieves 10 - 8  
Average 2.006 mm.

SAND SAMPLE NUMBER 6  
Magnification 10 diameters

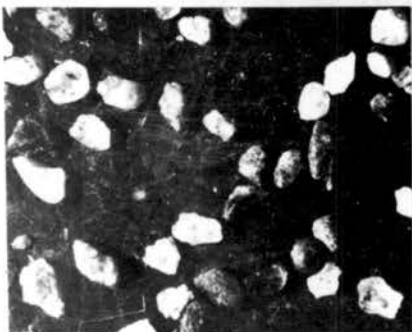
Type: River bed material  
Source: So. Fork Yuba River, Cisco, California



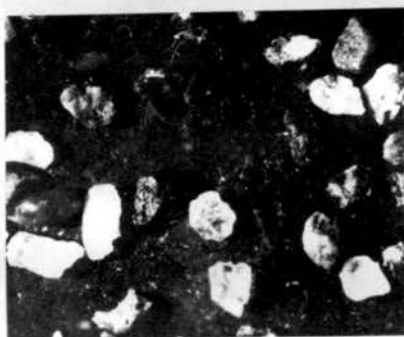
Tyler Sieves 65 - 60  
Average 0.227 mm.



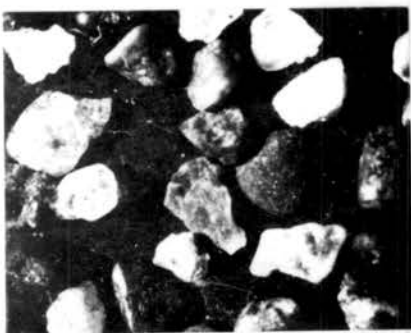
Tyler Sieves 60 - 48  
Average 0.270 mm.



Tyler Sieves 48 - 35  
Average 0.356 mm.



Tyler Sieves 35 - 28  
Average 0.503 mm.



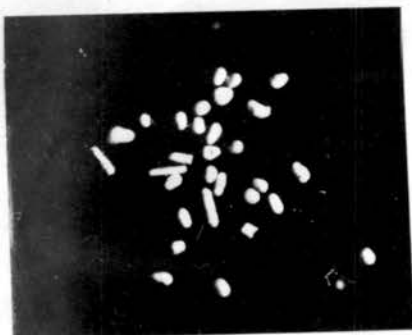
Tyler Sieves 28 - 20  
Average 0.712 mm.



Tyler Sieves 20 - 14  
Average 1.001 mm.

SAND SAMPLE NUMBER 7  
Magnification 10 diameters

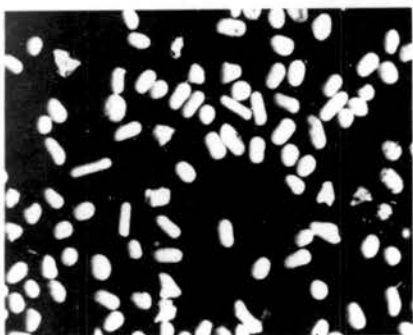
Type: River bed material  
Source: Putah Creek, Davis, California



Tyler Sieves 100 - 80  
Average 0.161 mm.



Tyler Sieves 80 - 65  
Average 0.192 mm.



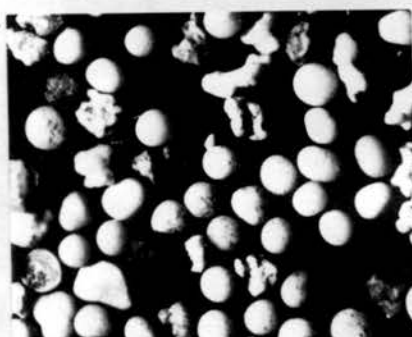
Tyler Sieves 65 - 60  
Average 0.227 mm.



Tyler Sieves 60 - 48  
Average 0.270 mm.



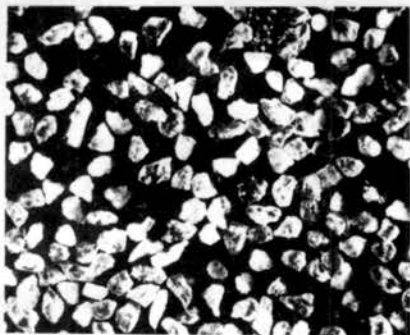
Tyler Sieves 48 - 35  
Average 0.356 mm.



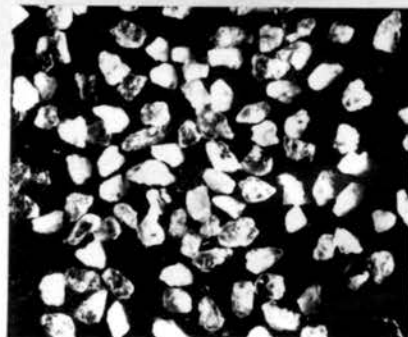
Tyler Sieves 35 - 28  
Average 0.503 mm.

SAND SAMPLE NUMBER 8  
Magnification 10 diameters

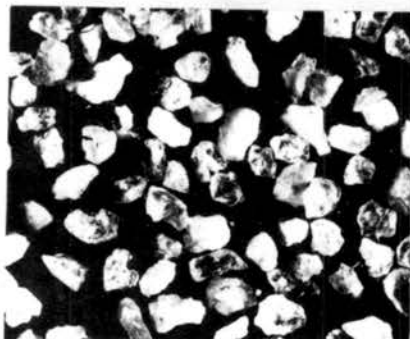
Type: Exceptionly well-worn dune sand  
Source: Dunes near Great Salt Lake, Utah



Tyler Sieves 65 - 60  
Average 0.227 mm.



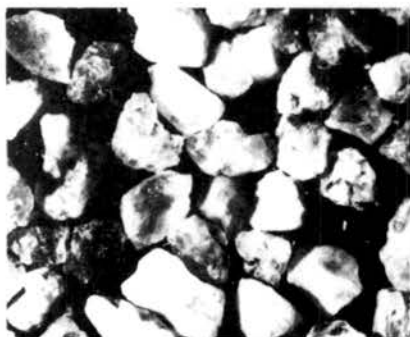
Tyler Sieves 60 - 48  
Average 0.270 mm.



Tyler Sieves 48 - 35  
Average 0.356 mm.



Tyler Sieves 35 - 28  
Average 0.503 mm.



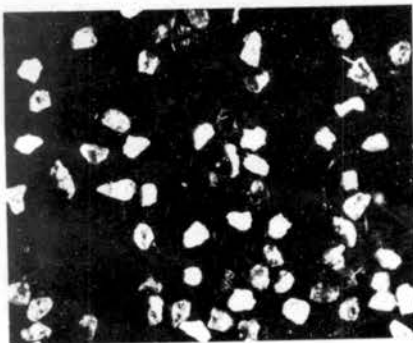
Tyler Sieves 28 - 20  
Average 0.712 mm.



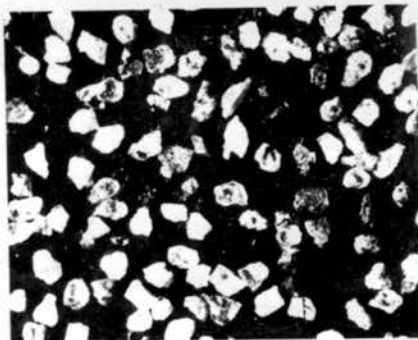
Tyler Sieves 20 - 14  
Average 1.001 mm.

SAND SAMPLE NUMBER 9  
Magnification 10 diameters

Type: Lake beach material  
Source: Grand Lake, Colorado



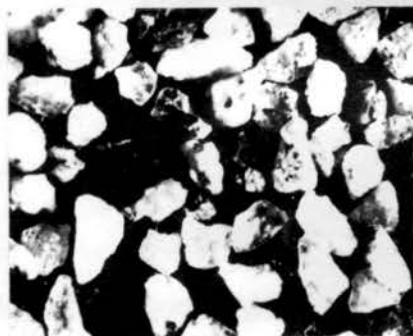
Tyler Sieves 65 - 60  
Average 0.227 mm.



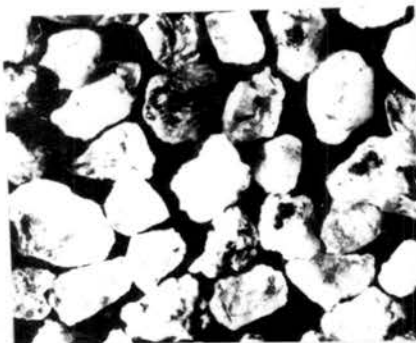
Tyler Sieves 60 - 48  
Average 0.270 mm.



Tyler Sieves 48 - 35  
Average 0.356 mm.



Tyler Sieves 35 - 28  
Average 0.503 mm.



Tyler Sieves 28 - 20  
Average 0.712 mm.



Tyler Sieves 20 - 14  
Average 1.001 mm.

SAND SAMPLE NUMBER 10  
Magnification 10 diameters

Type: River bed material  
Source: Cache la Poudre River, Chambers Lake,  
Colorado

Appendix D.--DEFINITIONS

## DEFINITIONS

- Drag coefficient.-- The coefficient in the drag force equation ( $F = C_D A \frac{\rho v^2}{2}$ ) expressing the relative resistance of bodies of the same cross-sectional area under the same flow conditions.
- Gravel.-- The class name for sediment of nominal diameters varying from 2 to 64 millimeters.
- Nominal diameter.-- The diameter of a sphere of the same volume as the given particle.
- Resistance curve.-- A line of points on the Reynolds number versus drag coefficient graph representing bodies of constant geometric shape.
- Reynolds number.-- The ratio of the inertia forces to the viscous forces acting on the particular body in the particular fluid.
- Sand.-- The class name for sediment of nominal diameters varying from 0.062 to 2.000 millimeters.
- Sediment.-- Fragmental material transported by suspended in, or deposited by water or air, or accumulated in beds by other natural agents. Floating organic material and ice are not included.
- Sedimentation diameter.-- The diameter of a sphere of the same terminal uniform settling velocity as the given particle in the same sedimentation fluid.
- Sieve diameter.-- The size of opening through which the given particle will just pass.
- Silt.-- The class name for sediment of nominal diameters varying from 0.004 to 0.062 millimeters.
- Sphericity.-- The ratio of a sphere of the same volume as the particle to the actual surface area of the particle.

Stokes equation.-- The theoretically developed expression for the terminal fall velocity of a sphere whose fall is dependent solely upon viscous effects.  $(v = \frac{1}{18} \frac{(\rho_s - \rho_f) g d^2}{\mu})$ .

Stokes range.-- The range of Reynolds number (all values up to about 0.1) for which Stokes equation is in agreement with experimental data.

oucher bond  
4-27-58  
RASHMONT

Appendix E.--NOTATION

## NOTATION

$A$  = nominal cross sectional area of the particle  
 $= \pi d_n^2/4$

$C_D$  = drag coefficient  
 $= \frac{4/3 (\rho_s - \rho_f) g d_n}{v_o^2 \rho_f} = 2F/A \rho_f v_o^2$

$d$  = sieve diameter

$d_n$  = nominal diameter

$d_o$  = sedimentation diameter

$F$  = force on the particle  
 $= \frac{\pi}{6} d_n^3 (\rho_s - \rho_f) g = C_D A \frac{\rho_f v_o^2}{2}$

$g$  = acceleration of gravity  
 $= 981$  centimeters per second

$\mu$  = dynamic viscosity of the fluid

$\nu$  =  $\frac{\mu}{\rho_f}$  = kinematic viscosity of the fluid

$R$  =  $\frac{\rho_f v_o d_n}{\mu}$  = Reynolds number

$\rho_s$  = solid density of the particle

$\rho_f$  = density of the fluid

$v_o$  = terminal uniform fall velocity

BIBLIOGRAPHY

RESEARCH LONG  
LIBRARY  
PUEBLO, COLO.

## BIBLIOGRAPHY

1. American Geophysical Union. Stream Dynamics Committee. Sub-committee on Sediment Terminology. Report, dated August 6, 1946. Fort Collins, Colo., Engineering Division, Colorado A & M College, 1947. 4 p. Mimeographed.  
Mimeographed for class use and not for distribution. Report signed by E. W. Lane, Chairman.
2. Otto, G. H. Comparative tests of several methods of sampling heavy mineral concentrates. Journal of sedimentary petrology, 3:30-39, April 1933.
3. Richards, R. H. Velocity of galena and quartz falling in water. American Institute of Mining Engineers. Transactions, 38:210-235, 1908.
4. Rouse, H. Elementary mechanics of fluids. New York, John Wiley and Sons, 1946. 411 p.
5. Rubey, W. W. Settling velocities of gravel, sand, and silt particles. American journal of science, 25:325-328, April 1933.
6. Tennessee Valley Authority. Methods of analyzing sediment samples. Iowa City, Ia., St. Paul U.S. Engineer District Sub-Office, Hydraulic Laboratory, University of Iowa, 1941. 203 p. Processed. (Its Study of methods used in measurement and analysis of sediment loads in streams. Report no. 4.)  
Planned and conducted jointly by Tennessee Valley Authority, Corps of Engineers, Department of Agriculture, Geological Survey, Bureau of Reclamation, Indian Service, and Iowa Institute of Hydraulic Research.
7. Wadell, H. Some practical sedimentation formulas. Geologiska Foreningen i Stockholm. Forhandlingar, 58:397-408, Maj-Okt., 1936.

8. Wadell, H. Volume, shape, and roundness of quartz particles. Journal of geology, 43:250-280, April-May 1935.
9. Zegrzda, A. P. Settling of gravel and sand grains in standing water. Leningrad, Nauchno-Issledovatekskii Institut Gidrotekhniki. Izvestiya, 12:50-54, 1934.  
Summary in English.